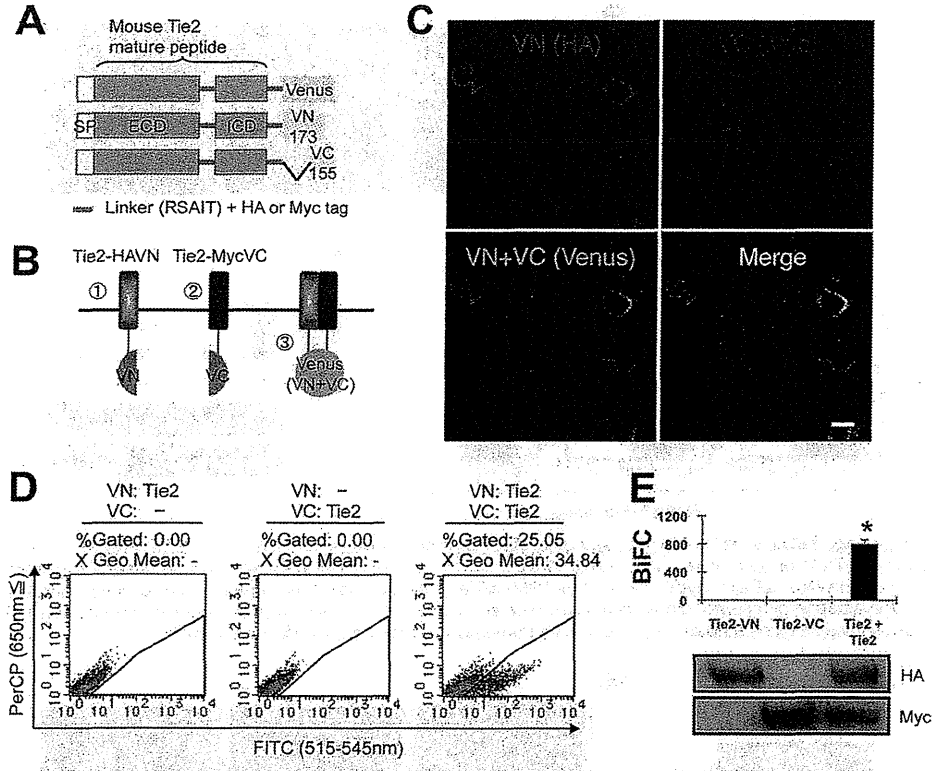

FIGURE 1. **BiFC analysis of Tie2 receptor homodimerization in living cells.** *A* and *B*, schematic representation of Tie2 tagged with either the N- or C-terminal of the Venus fragment (VN or VC). *SP*, signal peptide; *ECD*, extracellular domain; *ICD*, intracellular domain. When Tie2 dimerizes, fluorescence should reconstitute. *C*, HEK293T cells expressing Tie2-HAVN (*red*) and Tie2-MycVC (*blue*) observed by confocal microscopy. Cells were co-transefected with Tie2-HAVN and Tie2-MycVC expression vectors. Note that cells expressing Tie2-HAVN alone (*red arrowhead*) or Tie2-MycVC alone (*blue arrowhead*) develop no Venus fluorescence. *Bar* indicates 20 μm. *D*, flow cytometric analysis for evaluation of receptor dimerization as indicated. *E*, quantitative evaluation of Tie2 homodimerization in BiFC as observed in *D* (*, $p < 0.05$; $n = 3$). Protein expression level of each receptor was assessed by immunoblotting with anti-HA or anti-Myc Ab.

mouse anti-Myc Ab and Alexa Fluor 647 (blue)-conjugated anti-mouse Igs. BiFC fluorescence was detected using a filter for Alexa Fluor 488 (green). The slides were observed under a Leica TCS SP5 Ver1.6 (Leica Microsystems) using HCX PL APO lambda blue 63 × 1.4 oil. Images were processed using Adobe Photoshop CS5 Extended software (Adobe Systems).

Statistical Analysis—All data are displayed as the mean ± S.D. and were analyzed by two-tailed Student *t* test. A probability value of < 0.05 was considered statistically significant.

RESULTS

Establishment of Imaging Methods for Investigating the Dimerization of Tie2 Receptors—It has been reported that Tie2 is present in the form of dimers and/or oligomers on the cell surface (19). We also detected ligand-independent dimers of endogenous Tie2 in human umbilical vein endothelial cells (supplemental Fig. S1*A*). To assess Tie2 dimerization in the absence of Ang1, we utilized the BiFC assay (26). First, we prepared amino (N)-terminal (1–173: VN173) and carboxyl (C)-terminal (155–238: VC155) components of Venus fluorescent protein, a modifier of yellow fluorescent protein, fused with the C-terminal domain of wild-type (WT) mouse Tie2 with an HA or Myc tag linked to the molecule (Fig. 1*A*). When Tie2 (Tie2-HAVN, Tie2-MycVC) dimerizes, the fluorescent complex should be reconstituted (Fig. 1*B*). As expected, when Tie2-HAVN and Tie2-MycVC were cotransfected into HEK293T cells, cells expressing both HA and Myc developed fluorescence (Fig. 1*C*). Flow cytometry showed that transfection with both Tie2-HAVN and Tie2-MycVC vectors, but not with either alone, resulted in cells having high FITC intensity (Fig. 1, *D* and *E*). We confirmed that these co-transfectants developed BiFC fluorescence in cells expressing physiological levels of Tie2 as observed in ECs (supplemental Fig. S1, *B* and *C*).

Analysis of the Dimerization of Tie2-Tie1 using BiFC Assays—Ang1 activates Tie1 indirectly, mediated by its interaction with Tie2 (11, 12). It has been suggested that co-localization of Tie2 and Tie1 is induced upon activation of Tie2 by Ang1 (6). We investigated whether Tie2 and Tie1 also form heterodimers in a ligand-independent manner. Relative to Tie2, we found that the Tie1 protein was difficult to express in HEK293T cells following transfection of full-length Tie1 cDNA. However, when the original native signal sequence of Tie1 was excised and replaced with the Tie2 signal sequence (designated Tie1*), Tie1 expression was easily induced (Fig. 2*A*). Using this Tie1* construct, we evaluated Tie2-Tie1 and Tie1-Tie1 associations by BiFC. Although it has recently been reported that Tie2 and Tie1 associate following Ang1 stimulation and on cell-cell contact, we failed to detect any Tie2-Tie1 or Tie1-Tie1 associations (Fig. 2, *B–D*). This suggests that a Tie2 and Tie1 interaction is required for Ang1 binding to Tie2 and Tie1 and that Tie1 never gives rise to inactive dimers and/or oligomers in the absence of Ang1.

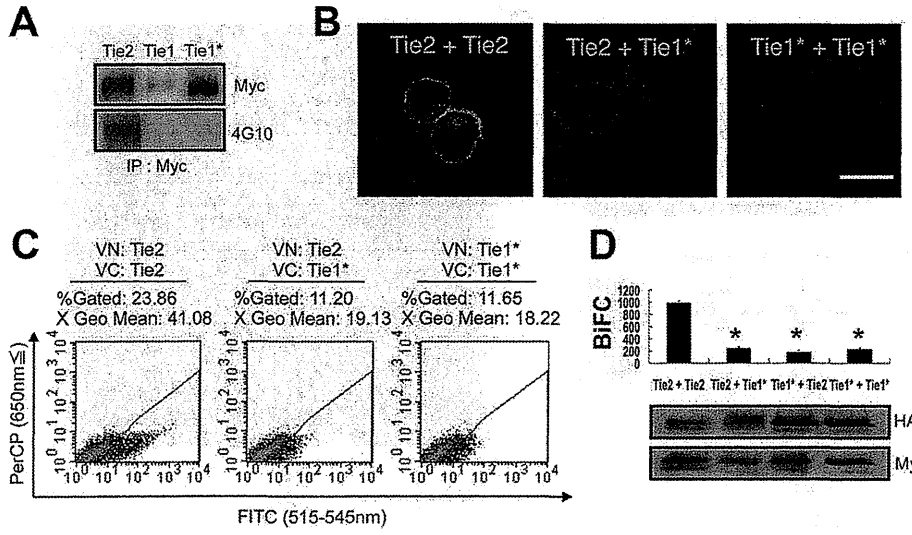

FIGURE 2. **BiFC analysis comparing Tie2 and Tie1*.** *A*, signal peptide of Tie1 was replaced with that of Tie2 (Tie1*). All receptors were C-terminally tagged with Myc. The levels of Tie2, Tie1, and Tie1* protein were analyzed with Myc or 4G10 Ab. *B–D*, HEK293T cells were transiently transfected in combination with Tie2-HAVN and Tie2-MycVC, Tie2-HAVN and Tie1*-MycVC, or Tie1*-HAVN and Tie1*-MycVC. *B*, cells were analyzed by confocal microscopy. *Bar* indicates 20 μm. *C*, flow cytometric analysis for evaluation of receptor dimerization as indicated. *D*, quantitative evaluation of receptor dimerization in BiFC as shown in *C* (*, $p < 0.05$; $n = 3$). Protein expression level of each receptor was assessed by immunoblotting with anti-HA or anti-Myc Ab.

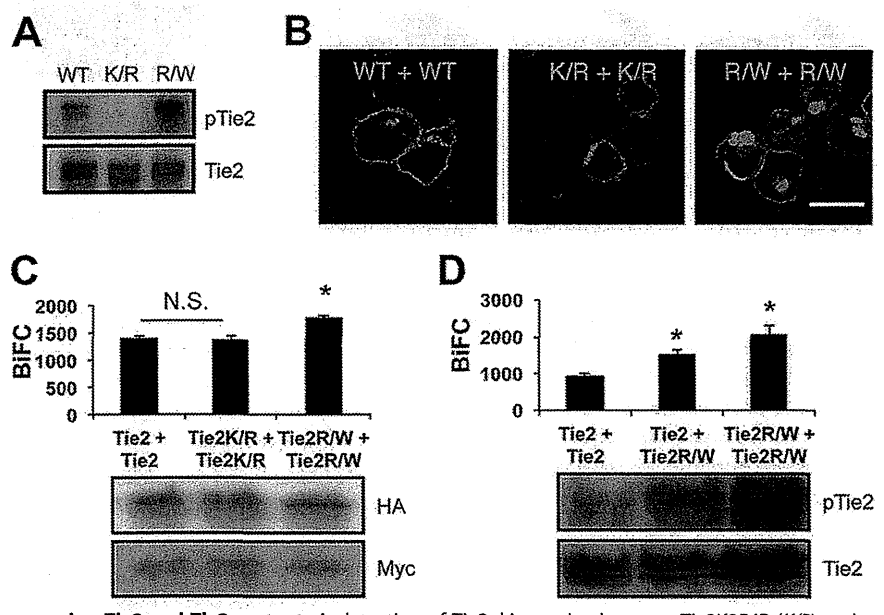

FIGURE 3. **BiFC analysis comparing Tie2 and Tie2 mutant.** *A*, detection of Tie2, kinase-dead mutant Tie2K854R (*K/R*) and constitutively active mutant Tie2R848W (*R/W*) phosphorylation. *B* and *C*, HEK293T cells were transiently transfected in combination with Tie2-HAVN and Tie2-MycVC, Tie2K854R-HAVN and Tie2K854R-MycVC, or Tie2R848W-HAVN and Tie2R848W-MycVC. *B*, cells were analyzed by confocal microscopy. *Bar* indicates 20 μm. *C*, quantitative evaluation of receptor dimerization in BiFC as shown in *B* (*, $p < 0.05$; $n = 3$). Protein expression level of each receptor was assessed by immunoblotting with anti-HA or anti-Myc Ab. *D*, quantitative evaluation of receptor dimerization in BiFC of Tie2 and Tie2R848W (*, $p < 0.05$; $n = 3$). Protein expression level of each receptor was assessed by immunoblotting with anti-Tie2. *N.S.*, not significant.

Analysis of the Dimerization of Tie2 Mutants Using BiFC Assays—Phosphorylation of overexpressed Tie1 and Tie2 was observed, but only Tie2 and not Tie1 was autophosphorylated in the absence of Ang1 stimulation (Fig. 2*A*). To test whether phosphorylation of Tie2 affects Tie2-Tie2 dimerization, we generated a kinase-inactive Tie2 mutant (Tie2K854R) (Fig. 3*A*). However, loss of phosphorylation did not affect Tie2 dimerization (Fig. 3, *B* and *C*, and supplemental Fig. S2A). We further confirmed that it was not until Ang1 bound Tie2 that dimerized Tie2 was internalized (supplemental Fig. S2*B*). Although dimerized WT Tie2 was observed in the cytoplasm, dimerized kinase-inactivated Tie2 did not internalize from the cell surface into the cytoplasm (Fig. 3*B*). Next, we constructed a constitutively active mutant of Tie2 (Tie2R848W) (Fig. 3*A*) (29). In HEK293T cells overexpressing Tie2R848W-HAVN and Tie2R848W-MycVC, more abundant Venus fluorescence was observed in the cytoplasm than in wt Tie2 or Tie2K854R (Fig. 3, *B* and *C*). Interestingly, Tie2R848W can dimerize with WT Tie2, resulting in BiFC intensity enhanced compared with Tie2-Tie2 dimers (Fig. 3*D*). These results suggest that our BiFC

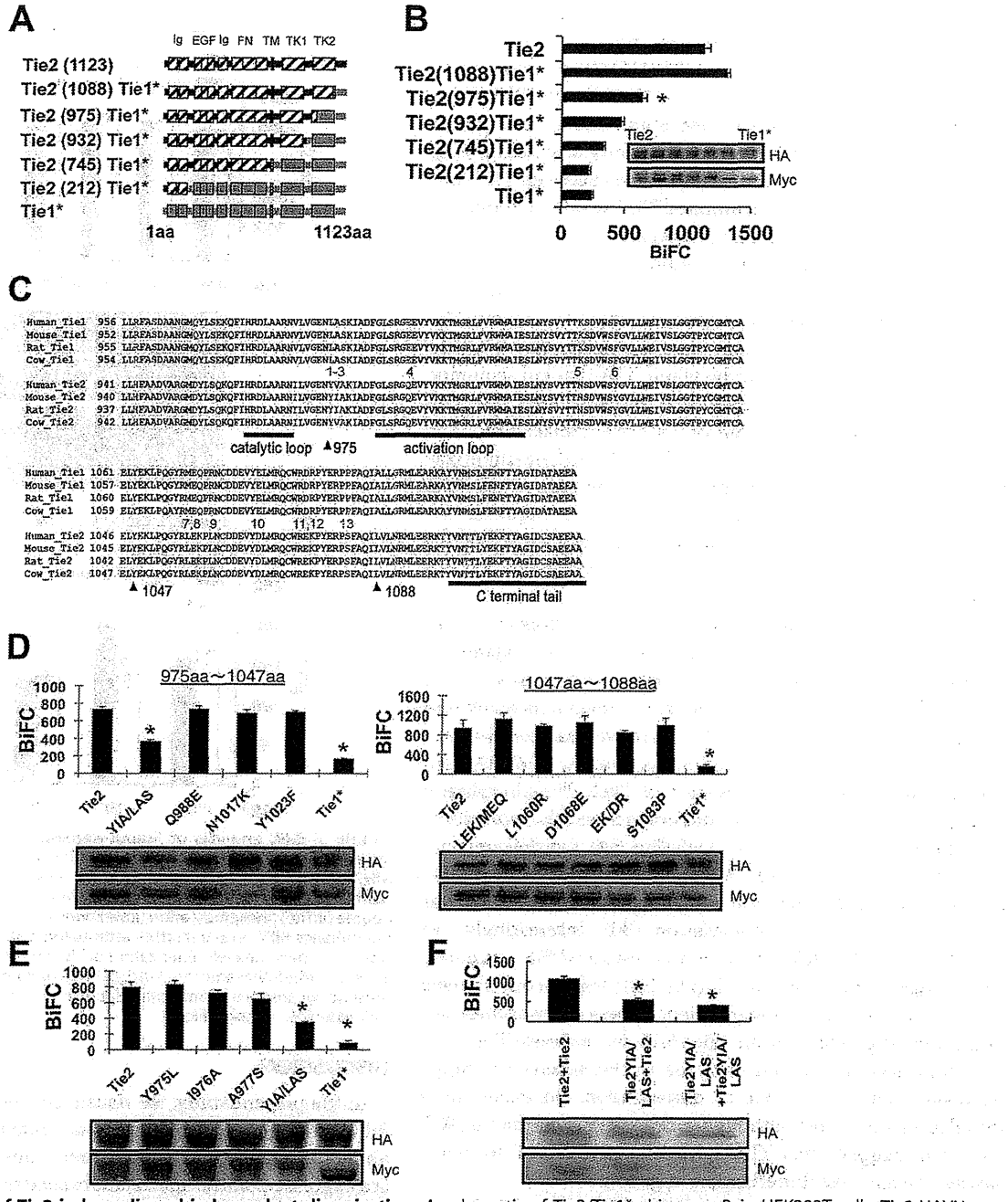

FIGURE 4. **YIA sequence of Tie2 induces ligand-independent dimerization.** *A*, schematic of Tie2/Tie1* chimeras. *B*, in HEK293T cells, Tie2-HAVN was transiently transfected in combination with Tie2, Tie2(1088)Tie1*, Tie2(975)Tie1*, Tie2(932)Tie1*, Tie2(745)Tie1*, Tie2(212)Tie1*, or Tie1* C-terminally fused with MycVC, and close associations of receptors assessed by BiFC and flow cytometry (*, $p < 0.05$; $n = 3$). The protein expression level of each receptor was confirmed by immunoblotting with anti-HA or anti-Myc Ab (*inset*). *C*, comparison of amino acid sequences of Tie1 and Tie2 C terminus from different species. *Pink*, different amino acids; *blue*, same amino acids (*aa*). *D* and *E*, in HEK293T cells, Tie2-HAVN was transiently transfected in combination with Tie2, Tie2YIA/LAS, Tie2Q988E, Tie2N1017K, Tie2Y1023F, Tie2LEK/MEQ, Tie2L1060R, Tie2D1068E, Tie2EK/DR, Tie2S1083P, or Tie1* C-terminally fused with MycVC (*D*) or Tie2, Tie2Y975L, Tie2I976A, Tie2A977S, Tie2YIA/LAS, or Tie1* C-terminally fused with MycVC (*E*), and close associations of receptors assessed by BiFC and flow cytometry. Protein expression level of each receptor was confirmed by immunoblotting with anti-HA or anti-Myc Ab (*inset*) (*, $p < 0.05$; $n = 3$). *F*, YIA domain of Tie2 was replaced by LAS sequence (Tie2YIA/LAS). Association of Tie2-Tie2, Tie2-Tie2YIA/LAS, and Tie2YIA/LAS-Tie2YIA/LAS was observed by BiFC as described above. Protein expression level of each receptor was confirmed by immunoblotting with anti-HA or anti-Myc Ab (*inset*) (*, $p < 0.05$; $n = 3$).

system mimics canonical receptor down-modulation only after activation of the receptor.

Identification of the Domain That Induces Ligand-independent Tie2 Homodimerization—We found that Tie2, but not Tie1, forms homodimers in a ligand-independent manner. Hence, we attempted to isolate the Tie2 ligand-independent dimerizing region. First, we sought domains responsible for Tie2-Tie2 association by replacing part of Tie2 with the Tie1 homologous domain (Fig. 4*A*). We found that lack of the extracellular domain of Tie2 did not affect BiFC (supplemental Fig. S3), suggesting that BiFC caused by Tie2-Tie2 interaction is mainly induced by the intracellular domain of Tie2 in our

model. Therefore, we focused on the intracellular domain of Tie2 for dimerization in our next experiments.

We transfected Tie2-HAVN and Tie2/Tie1* chimeric genes fused with Myc-tagged VC155 into HEK293T cells. When the C-terminal of Tie2 (from 975 to 1088 amino acids) was replaced by the Tie1 sequence, BiFC was significantly attenuated (Fig. 4*B*). There are differences in 13 amino acids between Tie2 and Tie1 (Fig. 4*C*). Therefore, we mutated Tie2 where its sequence is different from Tie1 domain by domain and observed Tie2-Tie2/mutant dimerization. We found that a YIA sequence within Tie2 (975–977) is critical for dimerization (Fig. 4*D*). Next, we introduced point mutations into this YIA domain. We found that no single mutation was responsible for reducing Tie2 dimerization, but rather the whole YIA tandem sequence was involved (Fig. 4*E*). We generated mutant Tie2 (Tie2YIA/LAS) in which the YIA domain of Tie2 was replaced by LAS. Tie2-Tie2YIA/LAS and Tie2YIA/LAS-Tie2YIA/LAS dimerization was not significantly different, suggesting that both Tie2 YIA domains in the cytoplasmic region are required for dimerization (Fig. 4*F*). When phosphorylation of Tie2YIA/LAS was assessed, it was found that mere overexpression did not induce it (supplemental Fig. S4).

Tie2YIA/LAS Monomer Mutants Can Be Dimerized and Phosphorylated by Ligand Binding—Tie2 can form ligand-independent inactive dimers; it has therefore been suggested that receptor dimerization and activation are mechanistically distinct and separable events (19, 30). Next, we analyzed whether Ang1 binding to the inactive monomer mutant Tie2YIA/LAS induced dimerization and activation of Tie2. Phosphorylation of WT Tie2 by exogenous Ang1 did not increase the intensity of BiFC developed by either Tie2-Tie2 (Fig. 5*A*). On the contrary, Ang1 stimulation decreased BiFC intensity after 30 min. This suggests that internalization and degradation of Tie2 was induced after Tie2 phosphorylation (30). Interestingly, we found that Tie2YIA/LAS prominently enhanced BiFC intensity under Ang1 stimulation for 1 h (Fig. 5*B*). Microscopy showed that Tie2 formed ligand-independent dimers and was internalized upon Ang1 stimulation (Fig. 6*A*). In contrast, Tie2YIA/LAS dimerization was not detected in the absence of Ang1. However, BiFC signals due to dimerization did occur upon stimulation with Ang1, although to a lesser extent than in WT Tie2. This suggests that YIA mutations in Tie2 did not completely prevent Tie2 dimerization (Fig. 6*B*).

Finally, we investigated how the lack of Tie2 ligand-independent dimerization affected its phosphorylation and downstream Erk signaling. When the time course of Tie2 phosphorylation was recorded in the presence of a fixed dose of Ang1 (200 ng/ml), no significant differences between wild-type Tie2 and Tie2YIA/LAS were observed (Fig. 7*A*). However, when phosphorylation was measured after stimulation for 10 min with different doses of Ang1, Tie2 and Erk phosphorylation by Tie2YIA/LAS decreased at a high dose (350~500 ng/ml) of Ang1 compared with wild-type Tie2 (Fig. 7, *B* and *C*). These findings suggest that the YIA domain of Tie2 is not indispensable for dimerization of Tie2 but is used for forming non-ligand-mediated dimerization of Tie2 to effectively react to a higher dose of Ang1.

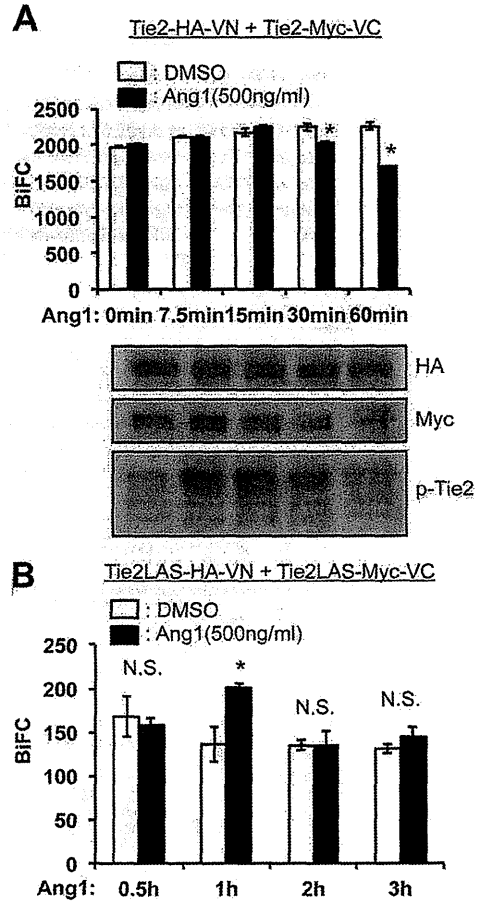

FIGURE 5. **BiFC analysis of ligand-dependent dimerization of Tie2.** *A*, dimerization of Tie2 was observed in Tie2-VN- and Tie2-VC-coexpressing NIH3T3 cells in the presence or absence of Ang1 stimulation. At each time point, cell lysates were analyzed for Tie2-HAVN and Tie2-MycVC as well as the degree of Tie2 phosphorylation (*lower panel*). Note that Ang1 stimulation did not enhance BiFC level but rather attenuated it 30 min after stimulation with Ang1. *B*, time course of dimerization of Tie2YIA/LAS (Tie2LAS) was observed in Tie2 YIA/LAS-VN- and Tie2 YIA/LAS -VC-coexpressing HEK293T cells in the presence or absence of Ang1 stimulation (*, $p < 0.05$; $n = 3$). *DMSO*, dimethyl sulfoxide; *N.S.*, not significant.

DISCUSSION

In the present study, we visualized Tie2 dimerization by the BiFC method and sought ligand-independent dimerization domains of Tie2. A previous report showed that Tie2 clusters are expressed on the apical and basolateral plasma membranes (19). However, it was not clear whether Tie2 phosphorylation results in dimer formation. Here, we showed that kinase-inactive Tie2 mutants also form dimers in the absence of Ang1. Thus, Tie2 can indeed form dimers without Ang1. To analyze the role of ligand-independent dimerization of Tie2, a mutant that cannot form dimers in the absence of Ang1 is required. In the present study, we utilized a mutant with no evidence of Tie1-Tie1 dimerization even when overexpressed. Based on the amino acid sequence difference between Tie2 and Tie1, we found that YIA in the Tie2 cytoplasmic domain is important for ligand-independent Tie2 dimerization.

We show that the YIA domain required to form ligand-independent Tie2 dimers is situated between the catalytic and activation loops in the intracellular region of the molecule. Previ-

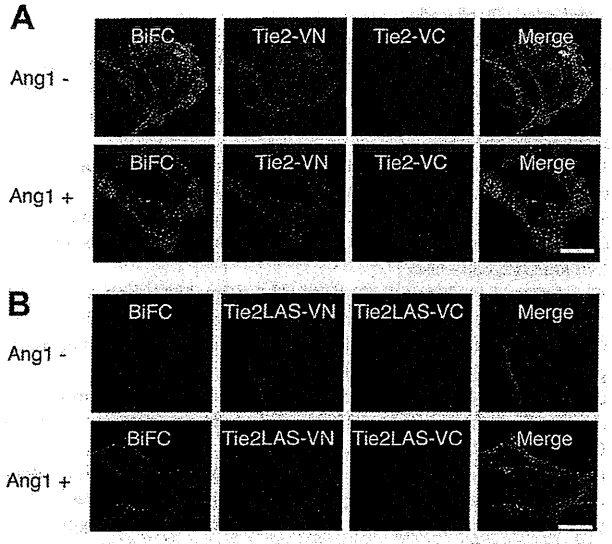

FIGURE 6. **Tie2YIA/LAS cannot form ligand-independent dimers but is dimerized and phosphorylated upon stimulation with Ang1.** *A*, dimerization and localization of Tie2 were observed in Tie2-VN- and Tie2-VC-coexpressing NIH3T3 cells in the presence or absence of Ang1. Wild-type Tie2 can form dimers irrespective of Ang1 stimulation, as confirmed by BiFC. However, this dimerized Tie2 forms cluster-like aggregations and is internalized upon stimulation with Ang1. *B*, similar to *A*, dimerization and localization of Tie2YIA/LAS (Tie2LAS) is observed in Tie2YIA/LAS-VN- and Tie2YIA/LAS-VC-coexpressing NIH3T3 cells. In the absence of Ang1, Tie2LAS did not dimerize but formed cluster-like aggregations upon stimulation with Ang1. *Bar* indicates 20 μm.

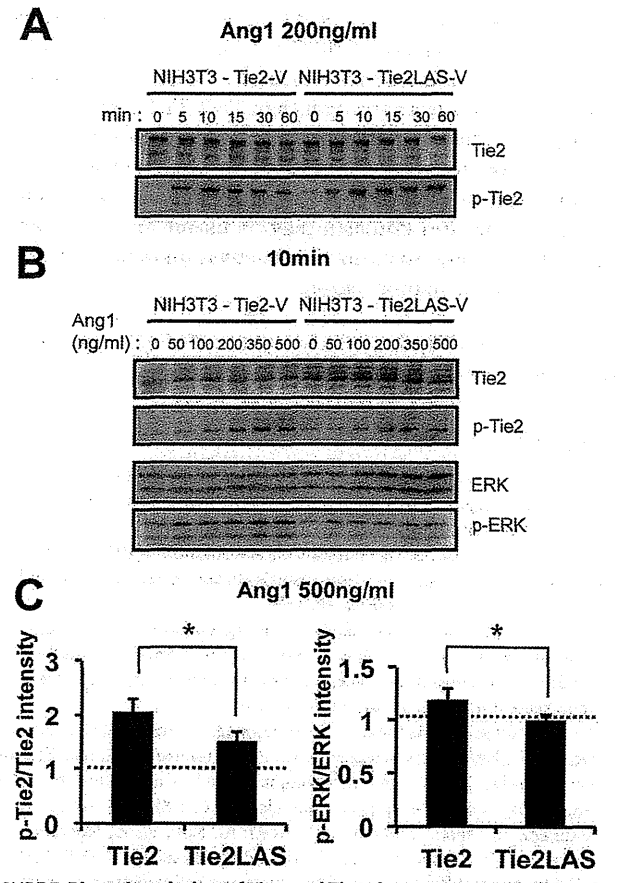

FIGURE 7. **Phosphorylation of Tie2 and Tie2 downstream molecule Erk.** *A*, Ang1 reactivity of Tie2 and Tie2YIA/LAS. After exposure to 200 ng/ml of Ang1, Tie2 and Tie2YIA/LAS phosphorylation was detected in a time-dependent fashion between 0 and 60 min. *B*, Ang1 reactivity of Tie2 and Tie2YIA/LAS. Ang1-mediated Tie2, Tie2YIA/LAS, and Erk phosphorylation was detected in a dose-dependent fashion between 0 and 500 ng/ml for 10 min. *C*, Tie2 and Erk phosphorylation on stimulation with 500 ng/ml Ang1 was quantified. The ratio of pTie2/Tie2 or pErk/Erk in cells on stimulation with Ang1 was compared with Ang1-untreated cells. (*, $p < 0.05$; $n = 3$).

ous reports show that the Tie2 C-terminal tail has a negative regulatory role in Tie2 signaling and function (31, 32). To activate Tie2, conformational changes in the intracellular loop structure and C-terminal tail are required for ATP and substrate binding. Therefore, it is possible that YIA domains control the movement of these loop and C-terminal tails. Further structural analysis of Tie2 will be necessary to assess how the YIA domain controls ligand-independent dimerization of Tie2 for folding and Tie2-Tie2 associations.

Unlike Tie2 homodimer formation, the BiFC method reveals that Tie2 and Tie1 scarcely interact. Recently, it has been reported that Tie2-Tie1 heterodimer formation is induced in the extracellular domain of Tie2 and Tie1, respectively, and that this occurs in the absence of angiopoietin ligation (33). Heterodimerization was observed using Tie receptors lacking intracellular domains. At present, it is difficult to explain this discrepancy, but it may simply be due to the absence of receptor cytoplasmic regions in the previous report. Indeed, when endogenous Tie2 and Tie1 localization in human umbilical vein endothelial cells was observed in the absence of Ang1, we found that Tie2 and Tie1 did not co-localize on the cell surface (supplemental Fig. S5). However, as previously reported, upon Ang1 stimulation, co-localization of these receptors does occur. In contrast, when NIH3T3 cells expressing Tie2-VN and Tie1*-VC were stimulated with Ang1, BiFC intensity was not enhanced (supplemental Fig. S6*A*). In addition, Ang1 activates both Tie2 and Tie1, but we did not observe a strong physical association between Tie2 and Tie1 in the immunoprecipitation analysis (supplemental Fig. S6, *B* and *C*). It has been reported that shedding of Tie1 extracellular domain itself induces Tie2 activation and that Ang2 acts as a Tie2 agonist upon Tie1 shedding (34–36). This suggests that Tie1 ectodomain shedding plays important roles in promoting Tie2 conformation changes and activation. Therefore, we cannot completely exclude the possibility that full-length Tie2 and Tie1 may heterodimerize under certain specific conditions in ECs.

It has been reported that Tie2 forms oligomers on the cell membrane (19); however, the function of such forms of Tie2 has not been elucidated. We found that a lack of ligand-independent dimerization of Tie2 led to attenuation of high dose Ang1-mediated activation of Tie2. This suggests that ligand-independent Tie2 dimerization plays a role in the rapid clustering of Tie2 upon activation with higher doses of Ang1 or in the preformation of Tie2 oligomers to respond to higher doses of Ang1. Further precise analysis of how ligand-independent dimerization of Tie2 relates to the extent of Tie2 phosphorylation at higher Ang1 doses is still required, including elucidation of the biological significance of Tie2 oligomers.

In humans, an amino acid substitution of tryptophan for arginine at residue (Tie2R849W) leads to ligand-independent constitutive activation; it is associated with familial venous malformations and causes thickness or lack of smooth muscle cells

in the veins systemically (14, 29, 37). In the present study, we showed that the intensity of BiFC signals from Tie2R848W-Tie2R848W was enhanced. Interestingly, Tie2R848W interactions with WT Tie2 were stronger than Tie2-Tie2 interactions. This suggests that Tie2R848W may heterodimerize with WT Tie2 and induce constitutive phosphorylation of WT Tie2. Therefore, analysis of regulatory mechanisms in ligand-independent dimerization domains may be useful for developing therapeutic strategies to inhibit Tie2 activation in patients suffering from venous malformation.

Acknowledgments—We thank T. Kamimoto, N. Fujimoto, and K. Fukuhara for technical assistance.

REFERENCES

1. Dejana, E., Tournier-Lasserve E., and Weinstein, B. M. (2009) The control of vascular integrity by endothelial cell junctions: molecular basis and pathological implications. *Dev. Cell* **16,** 209–221
2. Augustin, H. G., Koh, G. Y., Thurston, G., and Alitalo, K. (2009) Control of vascular morphogenesis and homeostasis through the angiopoietin-Tie system. *Nat. Rev. Mol. Cell Biol.* **10,** 165–177
3. Sato, T. N., Tozawa, Y., Deutsch, U., Wolburg-Buchholz, K., Fujiwara, Y., Gendron-Maguire, M., Gridley, T., Wolburg, H., Risau, W., and Qin, Y. (1995) Distinct roles of the receptor tyrosine kinases Tie-1 and Tie-2 in blood vessel formation. *Nature* **376,** 70–74
4. Davis, S., Aldrich, T. H., Jones, P. F., Acheson, A., Compton, D. L., Jain, V., Ryan, T. E., Bruno, J., Radziejewski, C., Maisonpierre, P. C., and Yancopoulos, G. D. (1996) Isolation of angiopoietin-1, a ligand for the TIE2 receptor, by secretion-trap expression cloning. *Cell* **87,** 1161–1169
5. Fukuhara, S., Sako, K., Minami, T., Noda, K., Kim, H. Z., Kodama, T., Shibuya, M., Takakura, N., Koh, G. Y., and Mochizuki, N. (2008) Differential function of Tie2 at cell-cell contacts and cell-substratum contacts regulated by angiopoietin-1. *Nat. Cell Biol.* **10,** 513–526
6. Saharinen, P., Eklund, L., Miettinen, J., Wirkkala, R., Anisimov, A., Winderlich, M., Nottebaum, A., Vestweber, D., Deutsch, U., Koh, G. Y., Olsen, B. R., and Alitalo, K. (2008) Angiopoietins assemble distinct Tie2 signalling complexes in endothelial cell-cell and cell-matrix contacts. *Nat. Cell Biol.* **10,** 527–537
7. Takakura, N., Watanabe, T., Suenobu, S., Yamada, Y., Noda, T., Ito, Y., Satake, M., and Suda, T. (2000) A role for hematopoietic stem cells in promoting angiogenesis. *Cell* **102,** 199–209
8. Dumont, D. J., Gradwohl, G., Fong, G. H., Puri, M. C., Gertsenstein, M., Auerbach, A., and Breitman, M. L. (1994) Dominant-negative and targeted null mutations in the endothelial receptor tyrosine kinase, tek, reveal a critical role in vasculogenesis of the embryo. *Genes Dev.* **8,** 1897–1909
9. Puri, M. C., Rossant, J., Alitalo, K., Bernstein, A., and Partanen, J. (1995) The receptor tyrosine kinase TIE is required for integrity and survival of vascular endothelial cells. *EMBO J.* **14,** 5884–5891
10. Puri, M. C., Partanen, J., Rossant, J., and Bernstein, A. (1999) Interaction of the TEK and TIE receptor tyrosine kinases during cardiovascular development. *Development* **126,** 4569–4580
11. Saharinen, P., Kerkelä, K., Ekman, N., Marron, M., Brindle, N., Lee, G. M., Augustin, H., Koh, G. Y., and Alitalo, K. (2005) Multiple angiopoietin recombinant proteins activate the Tie1 receptor tyrosine kinase and promote its interaction with Tie2. *J. Cell Biol.* **169,** 239–243
12. Yuan, H. T., Venkatesha, S., Chan, B., Deutsch, U., Mammoto, T., Sukhatme, V. P., Woolf, A. S., and Karumanchi, S. A. (2007) Activation of the orphan endothelial receptor Tie1 modifies Tie2-mediated intracellular signaling and cell survival. *FASEB J.* **21,** 3171–3183
13. Patan, S. (1998) TIE1 and TIE2 receptor tyrosine kinases inversely regulate embryonic angiogenesis by the mechanism of intussusceptive microvascular growth. *Microvasc. Res.* **56,** 1–21
14. Morris, P. N., Dunmore, B. J., Tadros, A., Marchuk, D. A., Darland, D. C., D'Amore, P. A., and Brindle, N. P. (2005) Functional analysis of a mutant form of the receptor tyrosine kinase Tie2 causing venous malformations. *J. Mol. Med.* **83,** 58–63
15. Maisonpierre, P. C., Suri, C., Jones, P. F., Bartunkova, S., Wiegand, S. J., Radziejewski, C., Compton, D., McClain, J., Aldrich, T. H., Papadopoulos, N., Daly, T. J., Davis, S., Sato, T. N., and Yancopoulos, G. D. (1997) Angiopoietin-2, a natural antagonist for Tie2 that disrupts *in vivo* angiogenesis. *Science* **277,** 55–60
16. Thomas, M., and Augustin, H. G. (2009) The role of the Angiopoietins in vascular morphogenesis. *Angiogenesis* **12,** 125–137
17. Eklund, L., and Olsen, B. R. (2006) Tie receptors and their angiopoietin ligands are context-dependent regulators of vascular remodeling. *Exp. Cell Res.* **312,** 630–641
18. Kim, I., Kim, J. H., Moon, S. O., Kwak, H. J., Kim, N. G., Koh, G. Y. (2000) Angiopoietin-2 at high concentration can enhance endothelial cell survival through the phosphatidylinositol 3′-kinase/Akt signal transduction pathway. *Oncogene* **19,** 4549–4552
19. Bogdanovic E., Coombs N., and Dumont D. J. (2009) Oligomerized Tie2 localizes to clathrin-coated pits in response to angiopoietin-1. *Histochem. Cell Biol.* **132,** 225–237
20. Jura, N., Endres, N. F., Engel, K., Deindl, S., Das, R., Lamers, M. H., Wemmer, D. E., Zhang, X., and Kuriyan, J. (2009) Mechanism for activation of the EGF receptor catalytic domain by the juxtamembrane segment. *Cell* **137,** 1293–1307
21. Red Brewer, M., Choi, S. H., Alvarado, D., Moravcevic, K., Pozzi, A., Lemmon, M. A., and Carpenter, G. (2009) The juxtamembrane region of the EGF receptor functions as an activation domain. *Mol. Cell* **34,** 641–651
22. Yu, X., Sharma, K. D., Takahashi, T., Iwamoto, R., and Mekada, E. (2002) Ligand-independent dimer formation of epidermal growth factor receptor (EGFR) is a step separable from ligand-induced EGFR signaling. *Mol. Biol. Cell* **13,** 2547–2557
23. Tao, R. H., and Maruyama, I. N. (2008) All EGF (ErbB) receptors have preformed homo- and heterodimeric structures in living cells. *J. Cell Sci.* **121,** 3207–3217
24. Livnah, O., Stura, E. A., Middleton, S. A., Johnson, D. L., Jolliffe, L. K., and Wilson, I. A. (1999) Crystallographic evidence for preformed dimers of erythropoietin receptor before ligand activation. *Science* **283,** 987–990
25. Chan, F. K., Chun, H. J., Zheng, L., Siegel, R. M., Bui, K. L., and Lenardo, M. J. (2000) A domain in TNF receptors that mediates ligand-independent receptor assembly and signaling. *Science* **288,** 2351–2354
26. Kerppola, T. K. (2006) Design and implementation of bimolecular fluorescence complementation (BiFC) assays for the visualization of protein interactions in living cells. *Nat. Protocols* **1,** 1278–1286
27. Morita, S., Kojima, T., and Kitamura, T. (2000) Plat-E: an efficient and stable system for transient packaging of retroviruses. *Gene Ther.* **7,** 1063–1066
28. Saitoh, T., Nakano, H., Yamamoto, N., and Yamaoka, S. (2002) Lymphotoxin-β receptor mediates NEMO-independent NF-κB activation. *FEBS Lett.* **532,** 45–51
29. Vikkula, M., Boon, L. M., Carraway, K. L., 3rd, Calvert, J. T., Diamonti, A. J., Goumnerov, B., Pasyk, K. A., Marchuk, D. A., Warman, M. L., Cantley, L. C., Mulliken, J. B., and Olsen, B. R. (1996) Vascular dysmorphogenesis caused by an activating mutation in the receptor tyrosine kinase TIE2. *Cell* **87,** 1181–1190
30. Bogdanovic, E., Nguyen, V. P., and Dumont, D. J. (2006) Activation of Tie2 by angiopoietin-1 and angiopoietin-2 results in their release and receptor internalization. *J. Cell Sci.* **119,** 3551–3560
31. Shewchuk, L. M., Hassell, A. M., Ellis, B., Holmes, W. D., Davis, R., Horne, E. L., Kadwell, S. H., McKee, D. D., and Moore, J. T. (2000) Structure of the Tie2 RTK domain: self-inhibition by the nucleotide binding loop, activation loop, and C-terminal tail. *Structure* **8,** 1105–1113
32. Niu, X. L., Peters, K. G., and Kontos, C. D. (2002) Deletion of the carboxyl terminus of Tie2 enhances kinase activity, signaling, and function. Evidence for an autoinhibitory mechanism. *J. Biol. Chem.* **277,** 31768–31773
33. Seegar, T. C., Eller, B., Tzvetkova-Robev, D., Kolev, M. V., Henderson, S. C., Nikolov, D. B., and Barton, W. A. (2010) Tie1-Tie2 interactions mediate functional differences between angiopoietin ligands. *Mol. Cell* **37,** 643–655
34. Yabkowitz, R., Meyer, S., Black, T., Elliott, G., Merewether, L. A., and Yamane, H. K. (1999) Inflammatory cytokines and vascular endothelial

growth factor stimulate the release of soluble tie receptor from human endothelial cells via metalloprotease activation. *Blood* **93,** 1969–1979

35. Marron, M. B., Singh, H., Tahir, T. A., Kavumkal, J., Kim, H. Z., Koh, G. Y., and Brindle, N. P. (2007) Regulated proteolytic processing of Tie1 modulates ligand responsiveness of the receptor-tyrosine kinase Tie2. *J. Biol. Chem.* **282,** 30509–30517
36. Singh, H., Milner, C. S., Aguilar Hernandez, M. M., Patel, N., and Brindle, N. P. (2009) Vascular endothelial growth factor activates the Tie family of receptor tyrosine kinases. *Cell Signal.* **21,** 1346–1350
37. Limaye, N., Wouters, V., Uebelhoer, M., Tuominen, M., Wirkkala, R., Mulliken, J. B., Eklund, L., Boon, L. M., and Vikkula, M. (2009) Somatic mutations in angiopoietin receptor gene TEK cause solitary and multiple sporadic venous malformations. *Nat. Genet.* **41,** 118–124

Identification of Vascular Endothelial Side Population Cells in the Choroidal Vessels and Their Potential Role in Age-Related Macular Degeneration

Taku Wakabayashi,[1,2] Hisamichi Naito,[1] Kazuhiro Takara,[1] Hiroyasu Kidoya,[1] Susumu Sakimoto,[1,2] Yusuke Oshima,[2] Kohji Nishida,[2] and Nobuyuki Takakura[1,3]

[1]Department of Signal Transduction, Research Institute for Microbial Diseases, Osaka University, Osaka, Japan
[2]Department of Ophthalmology, Osaka University Graduate School of Medicine, Osaka, Japan
[3]JST, CREST, Sanbancho, Chiyoda-ku, Tokyo, Japan

Correspondence: Nobuyuki Takakura, Department of Signal Transduction, Research Institute for Microbial Diseases, Osaka University, 3-1 Yamada-oka, Suita, Osaka 565-0871, Japan;
ntakaku@biken.osaka-u.ac.jp.

Submitted: May 2, 2013
Accepted: August 31, 2013

Citation: Wakabayashi T, Naito H, Takara K, et al. Identification of vascular endothelial side population cells in the choroidal vessels and their potential role in age-related macular degeneration. *Invest Ophthalmol Vis Sci.* 2013;54:6686-6693. DOI: 10.1167/iovs.13-12342

Purpose. The neovascular form of age-related macular degeneration (AMD) is characterized by the growth of abnormal new blood vessels from the choroid, termed choroidal neovascularization (CNV). The origin of the new vessels in CNV, however, has not been elucidated fully to our knowledge. The purpose of this study is to identify vascular endothelial side population (SP) cells in the preexisting choroidal vessels, and investigate their potential role in AMD.

Methods. We made single cell suspensions of freshly isolated mouse choroidal, retinal, and brain tissue by enzymatic digestion. Vascular endothelial SP cells were isolated using flow cytometry based on the ability to efflux the DNA-binding dye, Hoechst 33342, via ATP-binding cassette (ABC) transporters.

Results. In the choroid, 2.8% of $CD31^{+}CD45^{-}$ vascular endothelial cells (ECs) showed a typical SP staining pattern. They were not bone marrow–derived and possessed high colony-forming capacity in vitro. They proliferated during laser-induced CNV in vivo. In contrast, stereotypic SP staining pattern was not observed in retinal and brain ECs. Retinal and brain EC-SP cells included increased SP populations with less colony-forming capacity within the SP compartment, because they contained cells with and without proliferative potential. The latter still could efflux the dye due to high levels of ABC transporters, such as ABCB1a, ABCC4, and ABCC6.

Conclusions. The EC-SP cells in the choroid may represent vessel-residing endothelial stem/progenitor cells contributing mainly to angiogenesis, and may be useful for augmenting vascular regeneration or for developing new antiangiogenic therapy in AMD.

Keywords: angiogenesis, endothelial cell, stem cell, side population, choroid

Ocular neovascular diseases, including diabetic retinopathy and the neovascular form of age-related macular degeneration (AMD), are the most common cause of severe vision loss worldwide.[1–3] Diabetic retinopathy is characterized by retinal ischemia accompanied by abnormal neovessel growth from the retinal vessels (retinal neovascularization),[1] whereas neovascular AMD is attributed to abnormal neovessel growth from the choroidal vessels (choroidal neovascularization [CNV]).[2,3] Retinal neovascularization and CNV are caused either by angiogenesis, a process involving new vascular endothelial cell (EC) sprouting from preexisting blood vessels,[4] or by vasculogenesis, involving bone marrow (BM)-derived circulating endothelial progenitor cells (EPCs) contributing to the neovasculature.[5–8] However, recent studies have suggested that the contribution of EPCs to neovessel formation is not as marked as reported previously.[9–12] Therefore, the main cellular origin of new ECs seems to be the vascular ECs residing in the preexisting blood vessels during angiogenesis-based neovessel formation.[11]

Vascular ECs residing in the preexisting blood vessels have been regarded as cells possessing equal potential to produce ECs in response to the angiogenic stimuli VEGF and bFGF. However, we recently identified a small population of vascular endothelial stem/progenitor cells in the preexisting blood vessels, which may be a source of new ECs during angiogenesis.[13] These cells were isolated using flow cytometry based on the side population (SP) phenotype, a common feature of adult stem cells, including hematopoietic, epidermal, and muscle stem cells characterized by the ability to efflux the DNA-binding fluorescent dye, Hoechst 33342, via ATP-binding cassette (ABC) transporters.[14–16] In contrast to the majority of cells that accumulate Hoechst 33342, termed main population (MP) cells, SP cells appear as a discrete unstained population to the side of the MP cells in a flow cytometry density dot plot. An SP cell population within the vascular ECs (EC-SPs) has been isolated from blood vessels in limb muscle.[13] Compared to non–EC-SP cells, EC-SP cells possess high proliferative potential in vivo and in vitro, consistent with their stem cell properties. However, EC-SPs in the retinal and choroidal vessels, and their role in angiogenesis have not been identified to our knowledge. In addition, EC-SP cells in the brain also have not been investigated in detail. In our study, we compared EC-SP cells in

the choroidal, retinal, and brain vessels to identify the origin of angiogenesis in those vessels.

Materials and Methods

Mice

The C57BL/6 mice and C57BL/6-Tg (CAG-EGFP) mice (EGFP mice) that express green fluorescent protein (GFP) in all tissues were purchased from Japan SLC (Shizuoka, Japan). Mice 8 to 12 weeks of age were used for experiments. All animal experiments were conducted in accordance with the ARVO Animal Statement for the Use of Animals in Ophthalmic and Vision Research.

Cell Preparation

Mice were euthanized and eyes were extracted. Retinal tissue was removed gently from the RPE-choroid-sclera complex. Choroidal tissue subsequently was scraped off the sclera. The whole brain also was extracted from the same mice. Respective tissue was excised, minced, and digested with Dispase II (Godo Shusei Corp., Chiba, Japan), collagenase (Wako, Osaka, Japan), and type II collagenase (Worthington Biochemical Corp., Lakewood, NJ) at 37°C.[17] The digested tissue was passed through 40-μm filters to yield single cell suspensions. Erythrocytes were lysed with ACK buffer (0.15 M NH_4Cl, 10 mM $KHCO_3$, and 0.1 mM Na_2-EDTA).

Flow Cytometry

Hoechst staining was performed as described previously.[14] Briefly, cell surface antigen staining was performed, and cell suspensions were incubated with Hoechst 33342 (5 μg/mL; Sigma, St. Louis, MO) at 37°C for 90 minutes in Dulbecco's modified Eagle's medium (DMEM, 2% fetal calf serum, 1 mM HEPES; Sigma) at a concentration of 10^6 nucleated cells/mL in the presence or absence of verapamil (50 μmol/L; Sigma). Cell surface antigen staining was performed as described previously.[18] The monoclonal antibodies (mAbs) used in immunofluorescence staining were anti-CD45 and anti-CD31 mAbs (eBiosciences, San Diego, CA). Respective isotype controls (eBiosciences) were used as negative controls. Propidium iodide (PI, 2 μg/mL; Sigma) was added before fluorescence-activated cell sorting (FACS) analysis to exclude dead cells. The stained cells were analyzed and sorted by a SORP FACSAria (BD Biosciences, San Diego, CA), and data were analyzed using FlowJo Software (Treestar Software, San Carlos, CA).

EC Colony-Forming Assay

The 10^3 EC-SP or MP cells were seeded on 24-well plates and cocultured on OP9 stromal cells in RPMI (Sigma), supplemented with 10% fetal calf serum (FCS) and 10^{-5}M 2-ME (Gibco, Grand Island, NY).[19] Cells were cultured for 10 days and the number of colonies counted after immunostaining.

Immunofluorescence

The procedure for staining was as reported previously.[20] For immunofluorescence, anti-CD31 mAb (BD Biosciences) was used for staining, and anti-rat IgG Alexa Fluor 488 (Invitrogen, Carlsbad, CA) and biotin-conjugated polyclonal anti-rat Ig (Dako, Glostrup, Denmark) were used as the secondary antibodies. Biotinylated secondary antibodies were developed using ABC kits (Vector Laboratories, Burlingame, CA). Cell nuclei were visualized with Hoechst dye (Sigma). Samples were visualized using an Olympus IX-70 equipped with UPlanFI ×4/0.13 and LCPlanFI ×20/0.04 dry objectives (Olympus Corporation, Tokyo, Japan). Images were acquired and processed with Adobe Photoshop CS3 software (Adobe Systems, Inc., San Jose, CA). All images shown are representative of more than four independent experiments.

Quantitative RT-PCR (qRT-PCR)

RNA was extracted from $CD31^+CD45^-$ EC cells, $CD31^+CD45^-$ EC-SP cells, and $CD31^+CD45^-$ EC-MP cells from the brain, retina, and choroid, respectively, using an RNeasy Mini Kit (Qiagen, Hilden, Germany), and cDNA was generated using reverse transcriptase from the ExScript RT reagent Kit (Takara, Otsu, Japan) as described previously.[21] Real-time PCR was performed using a Stratagene Mx3000P (Stratagene, La Jolla, CA). The polymerase chain reaction was performed on cDNA using specific primers (Supplementary Table S1). Expression level of the target gene was normalized to the GAPDH level in each sample.

Laser-Induced CNV

The C57BL/6 mice were anesthetized as described previously.[22] A total of 20 photocoagulation lesions was made with a diode laser (150 mW, 0.05 seconds, 75 μm; Ultima 2000 SE; Lumenis, Santa Clara, CA) between the retinal vessels in a peripapillary distribution in each fundus. Production of a subretinal bubble at the time of laser treatment confirmed the disruption of Bruch's membrane. The $CD31^+CD45^-$ ECs from the choroid were obtained 6 days after the laser procedure. Proportions and numbers of EC-SP cells per choroid were analyzed and calculated. Controls were the choroid from the untreated eye, or choroid from normal wild-type mice.

Murine BM Transplantation Model

The 8- to 12-week-old C57BL/6 mice underwent BM transplantation from same-aged EGFP donors. Briefly, BM cells were obtained by flushing the tibias and femurs of age-matched donor EGFP mice. The transplantation was performed into C57BL/6 mice lethally irradiated with 10.0 Gy, by intravenous infusion of approximately 1×10^7 donor whole BM cells. At 24 weeks after transplantation, by which time BM of recipient mice was reconstituted, the mice were used for the experiments. The percent reconstitution of the BM was confirmed in all mice at the time of experiments.

Statistical Analysis

All data are presented as mean ± SEM. For statistical analysis, SigmaStat software (SPSS, Inc., Chicago, IL) was used. When two groups were compared, a 2-sided Student's *t*-test was used. A probability value of less than 0.05 was considered statistically significant.

Results

Identification of Endothelial SP Cells in the Choroid, Retina, and Brain

We performed Hoechst 33342 staining and flow cytometric analysis of cells isolated from normal mouse choroid, retina, and brain to identify EC-SP cells. In the choroid, among cells positive for the EC marker CD31 and negative for the hematopoietic cell (HC) marker CD45 ($CD31^+CD45^-$ ECs, Fig. 1A), 2.8 ± 0.14% showed a typical SP staining pattern (i.e., Hoechst 33342 dye efflux properties, lost in the presence of the drug efflux pump inhibitor, verapamil, Fig. 1B). They were

Investigative Ophthalmology & Visual Science

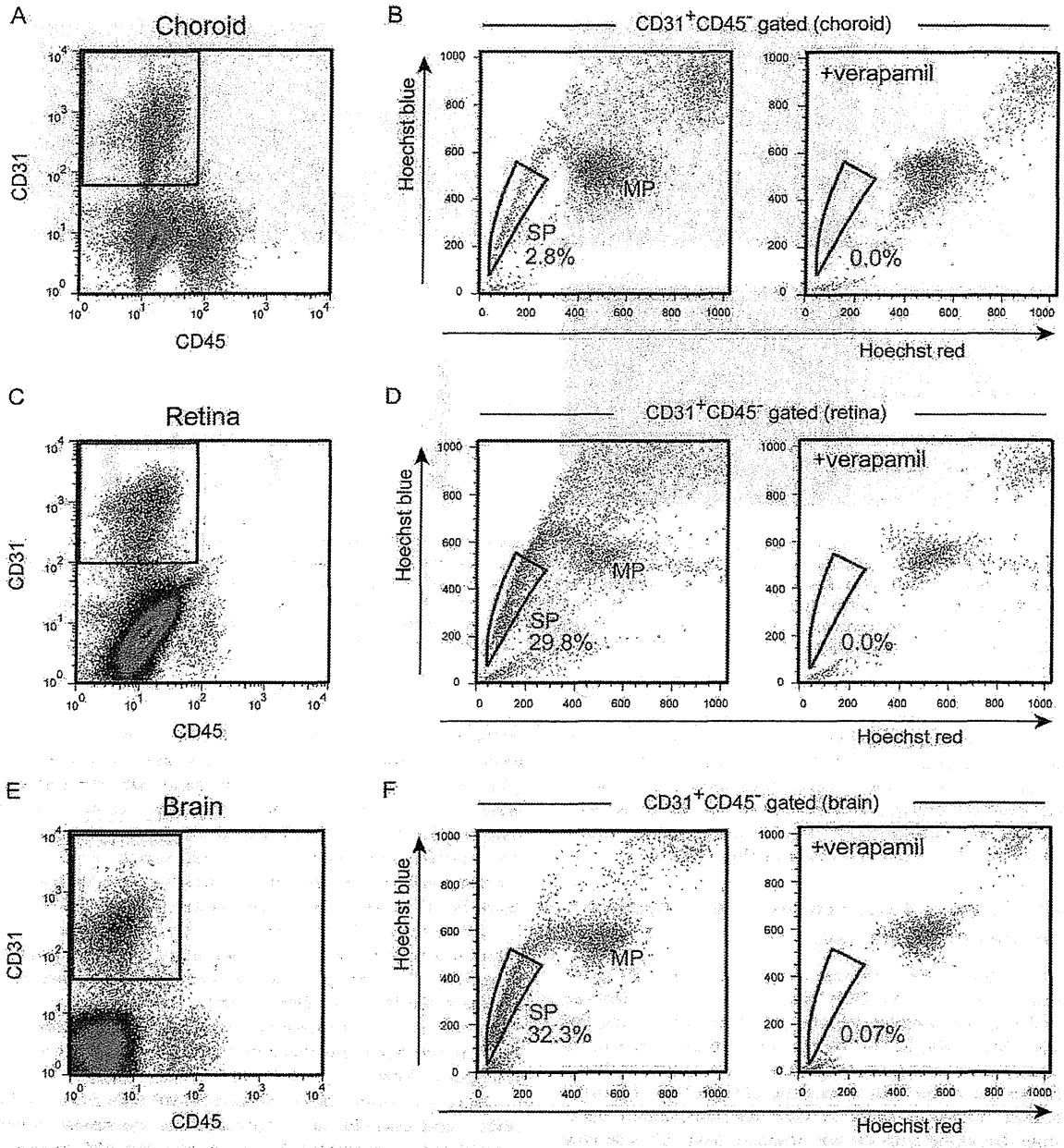

FIGURE 1. Identification of endothelial side population cells in the choroid, retina, and brain. (A) Flow cytometric analysis of choroidal ECs from wild-type mice. (B) Hoechst 33342 staining of $CD31^+CD45^-$ ECs gated as shown in (A). Of the cells, 2.8 ± 0.14% were in the SP gate. Note that verapamil selectively prevents Hoechst exclusion from EC-SP cells. (C) Flow cytometric analysis of retinal ECs from wild-type mice. (D) Of the cells, 29.8 ± 2.2% were in the SP gate. Note that a typical EC-SP pattern is not observed. (E) Flow cytometric analysis of brain ECs from wild-type mice. (F) Of the cells, 32.5 ± 2.6% were in the SP gate. Note the similar SP pattern as in the retina. Verapamil selectively prevents Hoechst exclusion from EC-SP cells.

distinct from the MP cells. On the other hand, the stereotypic SP staining pattern was not observed, and a higher proportion of SP cells were identified among $CD31^+CD45^-$ ECs from retina and brain compared to the choroid. Indeed, 29.8 ± 2.2% were in the SP gate in the retinal ECs (Fig. 1C) and 32.5 ± 2.6% in the brain (Fig. 1E). These cells also possessed Hoechst 33342 dye efflux properties, which disappeared in the presence of verapamil (Figs. 1D, 1F).

Proliferation and Colony-Forming Capacity of EC-SP Cells In Vitro

To evaluate the proliferative capacity of EC-SP cells in vitro, sorted EC-SP cells isolated from the choroid, retina, and brain were cultured on OP9 stromal cells, which support EC growth.[15] After 10 days, EC-SP cells isolated from the choroid generated a higher number of EC colonies compared to EC-MP cells (Fig. 2A). Each colony had a cord-like

Investigative Ophthalmology & Visual Science

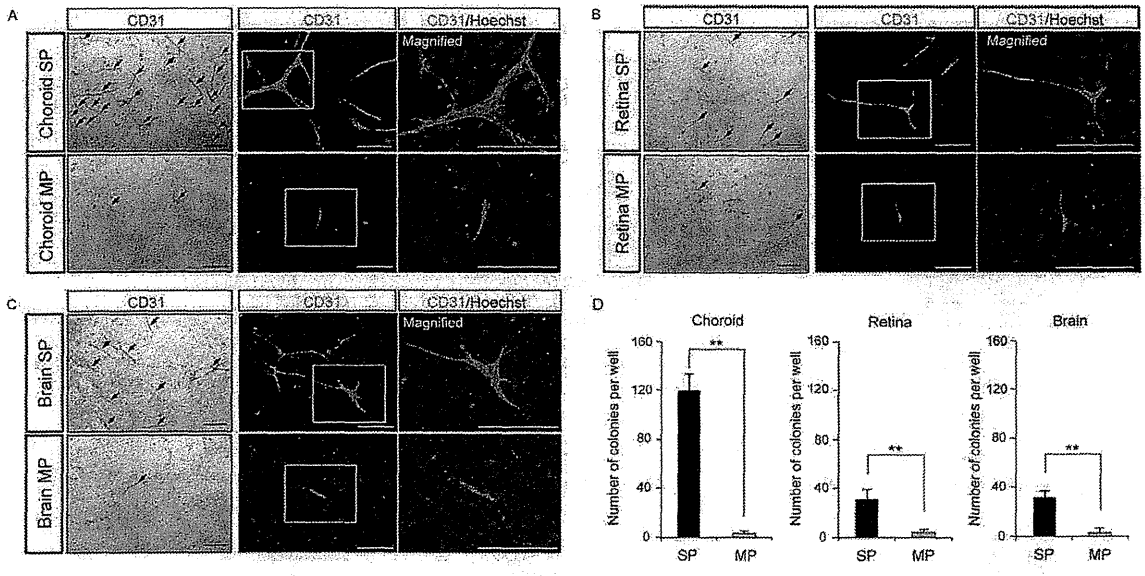

FIGURE 2. Endothelial SP cells in the choroid have high EC colony-forming ability. (**A**) EC-SP cells (*upper*) and EC-MP cells (*lower*) in the choroid were cultured on OP9 feeder cells and stained with anti-CD31 mAb. *Arrows* on the *left* image indicate each colony. Images on the *right* show a higher magnification of the areas indicated by boxes in the *middle* image. Note that EC-SP cells generate many CD31-positive EC colonies compared to EC-MP cells. Endothelial colony formation by EC-SP cells, or EC-MP cells from retina (**B**) or brain (**C**). Note that EC-SP cells (*upper*) in the retina (**B**) and brain (**C**) form many colonies, compared to EC-MP cells (*lower*), but the difference is less prominent compared to the choroid. (**D**) Quantitative evaluation of the number of CD31-positive ECs in one well of a 24-well culture dish. *Error bars* are ±SEM. $^{**}P < 0.01$ ($n = 4$). *Scale bars*: 500 μm.

structure, and included multiple ECs, as confirmed by CD31 and Hoechst staining. The EC-SP cells isolated from the retina and brain also formed higher numbers of ECs with a cord-like structure compared to respective EC-MP cells (Figs. 2B, 2C), but had substantially lower colony-forming ability than the EC-SP cells from the choroid (Fig. 2D).

EC-SP Cells Are Not Derived From Bone Marrow, and Are Distinct From EPCs

To confirm that EC-SP cells are not identical to EPCs, we transplanted BM cells from GFP mice into irradiated wild-type mice. Although the average percent reconstitution of the BM was more than 99% at 24 weeks after transplantation, as confirmed by flow cytometry (Figs. 3A–C), we could not detect any GFP-positive EC-SP cells among the $CD31^{+}CD45^{-}$ ECs from the choroid, retina, or brain of GFP BM-transplanted mice, suggesting that EC-SP cells do not originate from EPCs derived from BM (Figs. 3A–C). This indicates that EC-SP cells reside at the preexisting vessels in each tissue.

Expression of ABC Transporters in Choroidal, Retinal, and Brain ECs

Because the retinal and brain ECs had high proportions of EC-SP cells, but less efficient colony-forming capacity compared to choroidal ECs, we hypothesized that not only the stem cell–like ECs, but also nonstem cell–like ECs in the retina and brain also express high levels of ABC transporters constitutively to maintain the blood-retinal barrier (BRB) or blood-brain barrier (BBB). Therefore, we compared the ABC transporter gene family mRNA expression in choroidal, retinal, and brain ECs. Retinal and brain ECs showed similar expression patterns of several ABC transporters except for ABCC3 (Fig. 4). The expression levels of ABCB1a (multiple drug resistance 1a [MDR1a]), ABCA5, ABCC4, and ABCC6 were significantly higher in retinal and brain ECs compared to choroidal ECs (Figs. 4B, 4E, 4I, 4J). On the other hand, ABCB1b and ABCA9 were lower in retinal and brain ECs (Figs. 4C, 4G), indicating that they are not associated with an SP phenotype in these ECs. The relative expression of ABCG2, which is reported to correlate with the SP phenotype, was found to be high in the brain ECs (Fig. 4A). ABCG2 also tended to be highly expressed in the retinal ECs compared to choroidal ECs, but the difference was not statistically significant (Fig. 4A). These data suggested that components of the ABC transporters that maintain the BBB and BRB generally are similar, but different from the ECs in the choroid, which are distinguished from those in the brain and retina by the expression pattern of ABC transporter genes.

Next, we sorted the EC-SP and EC-MP cells from the brain, retina, and choroid, and compared the expression levels of several ABC transporters (Fig. 5). Among the ABC transporters that were highly expressed in the brain and retinal ECs relative to choroidal ECs (ABCG2, ABCB1a, ABCA5, ABCC4, and ABCC6), the expression of ABCB1a, ABCC4, and ABCC6 was significantly higher in retinal and brain EC-SP cells compared to choroidal EC-SP cells. This indicated that approximately 30% of ECs with the SP phenotype in the brain and retina express much higher levels of certain ABC transporters than choroidal stem-like EC-SP cells. Furthermore, the expression of ABCC4 and ABCC6 was significantly higher even in EC-MP cells in the retina and brain compared to choroidal EC-SP cells (Figs. 5D, 5E). The high levels of ABC transporters in the retinal and brain EC-MP cells also may contribute to maintaining the BRB or BBB. Such a specific role of ECs in the retina and brain may be the reason why the SP analysis using the Hoechst method does not work well enough to allow purification of the stem-like cells with proliferative potential from retinal and brain ECs.

Investigative Ophthalmology & Visual Science

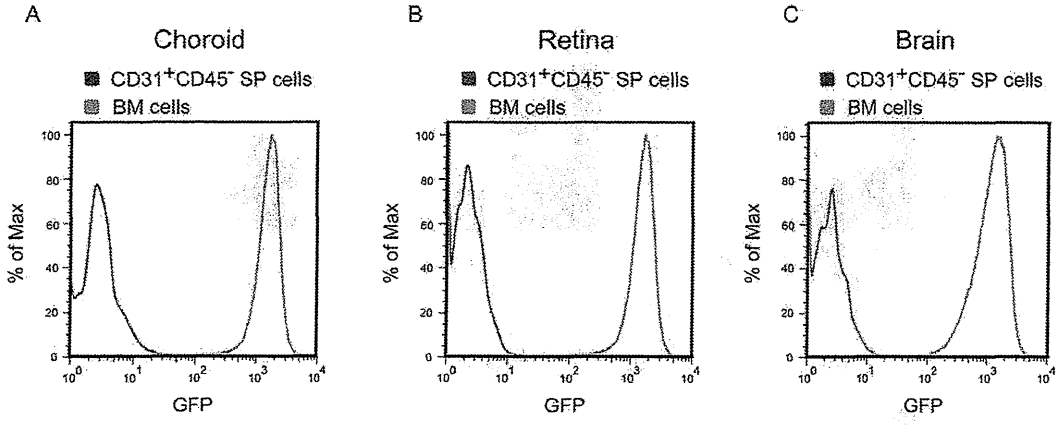

FIGURE 3. EC-SP cells are not derived from BM. (A–C) BM cells from GFP mice were transplanted into lethally-irradiated wild-type mice. At 24 weeks after transplantation, cells from the choroid (A), retina (B), and brain (C) were analyzed. Histogram showing GFP intensity of the $CD31^+CD45^-$ EC-SP fraction (*red*) and BM (*green*) obtained from the choroid, retina, and brain. Almost all BM cells were GFP-positive after transplantation. Note that GFP-positive $CD31^+CD45^-$ EC-SP cells were present at <0.01% of the total, suggesting no major contribution of BM cells to EC-SP cells.

EC-SP Cells in the Choroid Are Activated in Laser-Induced CNV

To study the potential of the EC-SP cells in the choroid to facilitate neovascularization in vivo, we investigated their proliferation during laser-induced CNV. A sham operation did not have any effect on the percentage of choroidal EC-SP cells (Figs. 6A, 6B). However, the percentage and absolute number of EC-SP cells in the choroid increased 6 days after laser treatment (Figs. 6C–F), while the percentage of brain and retinal EC-SP cells did not differ significantly after laser treatment (29.7 ± 2.9%, $P > 0.05$ and 32.6 ± 2.8%, $P > 0.05$ in retina and brain, respectively). These results suggested that a population of EC-SP cells in the choroid is maintained in the steady-state, but actively proliferates in response to angiogenic stimuli.

To investigate whether the EC-SP cells that had proliferated after laser treatment are BM-derived, BM cells from GFP mice were transplanted into lethally-irradiated wild-type mice, and CNV was induced by the laser 24 weeks after transplantation. No GFP-positive cells were present in the $CD31^+CD45^-$ EC-SP population even after CNV developed, indicating no major contribution of BM cells to the EC-SP cells that proliferated (Fig. 6G). Thus, EC-SP cells already present at the preexisting vessels seem to proliferate themselves in laser-induced CNV.

DISCUSSION

In our study, we identified resident EC-SP cells in the choroidal, retinal, and brain vessels. Choroidal EC-SP cells represented 2.8% of total ECs in the choroid and had greater colony-forming potential than the majority of the EC population. The pattern of SP phenotype and colony-forming potential of the choroidal EC-SP cells was similar to the recently reported EC-SP cells isolated from limb muscle.[13] Because EC-SP cells in the limb

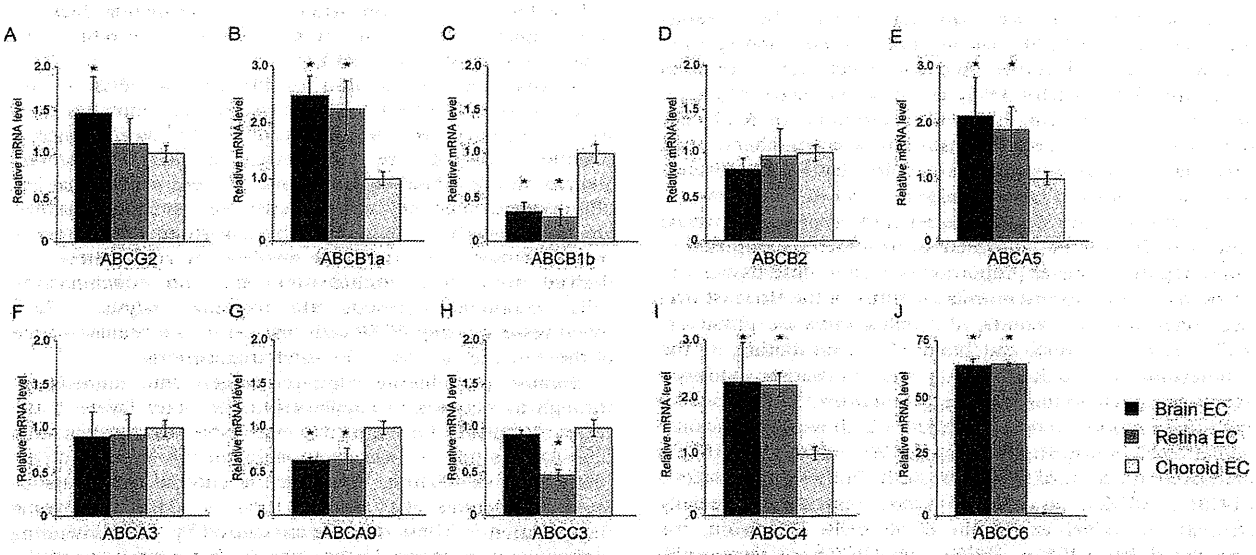

FIGURE 4. Quantitative RT-PCR analysis of mRNA in the choroidal, retinal, and brain EC. (A–J) Expression levels of ABC transporters in the choroidal, retinal, and brain $CD31^+CD45^-$ EC. Results are shown as fold-increase in comparison with choroidal ECs. Note that expression levels of ABCB1a, ABCA5, ABCC4, and ABCC6 were significantly higher in the retinal and brain ECs compared to choroidal ECs. *Error bars* are ±SEM. *$P < 0.05$ ($n = 4$).

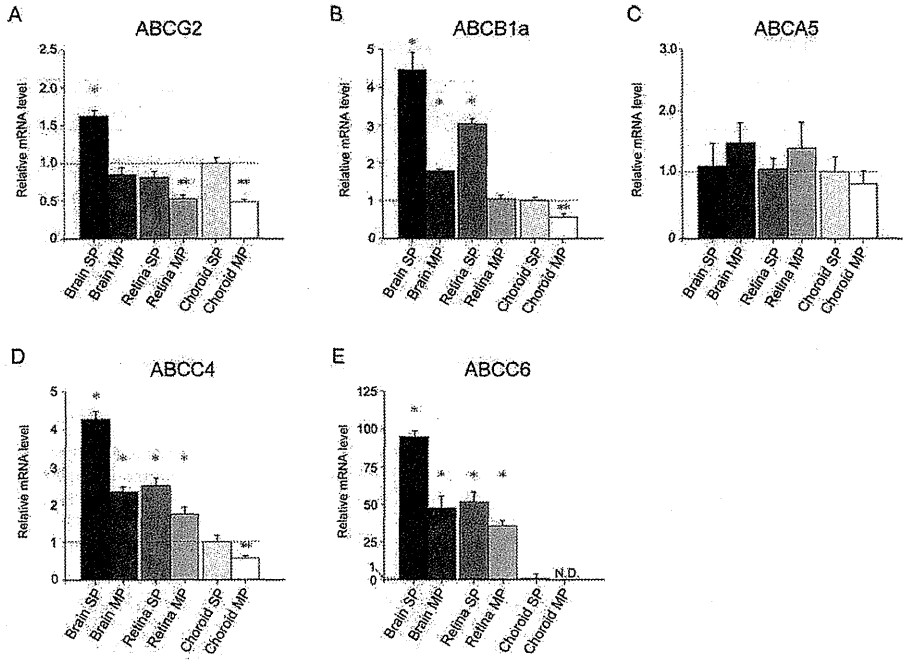

FIGURE 5. Quantitative RT-PCR analysis of mRNA in EC-SP and EC-MP cells from the choroid, retina, and brain. (A–E) Comparison of the expression levels of five ABC transporters that were highly expressed in retinal and brain ECs than choroidal ECs, as shown in Figure 4. Results are shown as fold-increase in comparison with choroidal EC-SP cells. ABCB1a, ABCC4, and ABCC6 were significantly higher in the brain and retinal EC-SP cells compared to choroidal EC-SP cells, potentially reflecting the high proportion of SP cells in the former. The ABCC4 and ABCC6 expression was significantly higher even in retinal and brain EC-MP cells compared to choroidal EC-SP cells. *Error bars* are ±SEM. Significantly higher ($^*P < 0.05$) and lower ($^{**}P < 0.05$) than choroidal EC-SP cells ($n = 3$).

muscle are regarded as colony-forming stem/progenitor-like ECs and termed "spEC" (to indicate specific ECs consisting of a hierarchical system of vascular ECs in the blood vessel), EC-SP cells from the choroid also may act as "spEC" in the choroidal vasculature.

The EC-SP cells in the choroid formed endothelial colonies positive for CD31 in culture, but did not give rise to cells other than ECs, such as hematopoietic or smooth muscle actin (SMA)–positive mural cells (data not shown). These results indicated that the EC-SP cells are lineage-committed specific ECs with high proliferative potential, which can be purified efficiently using Hoechst 33342 and flow cytometry. Although we could not investigate the in vivo contribution of EC-SP cells to choroidal angiogenesis, because of the small number of such cells that could be isolated, it is possible that EC-SP cells also have the potential to generate large number of ECs in vivo.

In contrast to the SP pattern seen in the choroid, the retinal and brain EC-SP cells contained an increased SP population, indicating that a higher proportion of ECs in those tissues can carry out ABC transporter-mediated efflux of the Hoechst dye. According to earlier reports, ABC transporters are physiologically active in retinal and brain ECs, contributing to the maintenance of barrier function and preventing cytotoxic agents from penetrating into the parenchyma.[23–25] Consistent with these reports, retinal and brain ECs showed significantly higher levels of ABCB1a (MDR1a), ABCA5, ABCC4, and ABCC6 compared to choroidal ECs in our study. Of these transporters, ABCB1a, ABCC4, and ABCC6 were expressed especially strongly in retinal and brain EC-SP cells. Therefore, we speculated that ABCB1a, ABCC4, and ABCC6 are responsible for the increase of the SP phenotype in retina and brain ECs. Because the expression levels of ABCC4 and ABCC6 were high even in retinal and brain EC-MP cells compared to choroidal EC-SP cells, EC-MP cells in the retina and brain also seemed to contribute to maintaining the BRB and BBB.

In addition to the different EC-SP pattern, EC-SP cells in the retina and brain had substantially less colony-forming potential compared to those in the choroid. Therefore, EC-SP cells in the retina and brain seemed to contain cells with as well as those without stem cell-like proliferative potential, but which still can efflux dye, leading to a lower proportion of stem cell-like cells within the EC-SP compartment. Thus, SP analysis does not work enough to purify the stem-like cells in the retinal and brain ECs as in the choroidal ECs.

Because the contribution of BM-derived EPCs to the formation of adult blood vessels in the eye and brain has been well-documented over the past decade,[7,8,26–29] we investigated whether EC-SP cells are of BM origin or not. Based on the analysis of GFP$^+$ BM-transplanted mice, where we saw that EC-SP cells were completely GFP-negative, we concluded that they are not BM-derived. This result is consistent with a recent report showing that the cells involved in angiogenesis are derived from local, nonhematopoietic, and noncirculating cells, according to genetic fate mapping analysis.[11] Thus, blood vessel-residing EC-SP cells may serve as a cellular source of the new ECs necessary for adult angiogenesis.

Because the choroid supplies oxygen and nourishment through its network of capillaries to the outer layers of the retina responsible for vision, it is reasonable that resident stem cell-like ECs may be present to maintain the integrity of the physiologic vasculature. However, the choroid also is associated with serious eye diseases, such as AMD and myopic degeneration.[2,3] These diseases are caused by CNV, generating pathologic new vessels in the choroid that grow beneath the retina. Because the EC-SPs have the potential to generate large numbers of ECs, we hypothesized that EC-SP cells may contribute to CNV in vivo. Using a laser-induced experimental

Investigative Ophthalmology & Visual Science

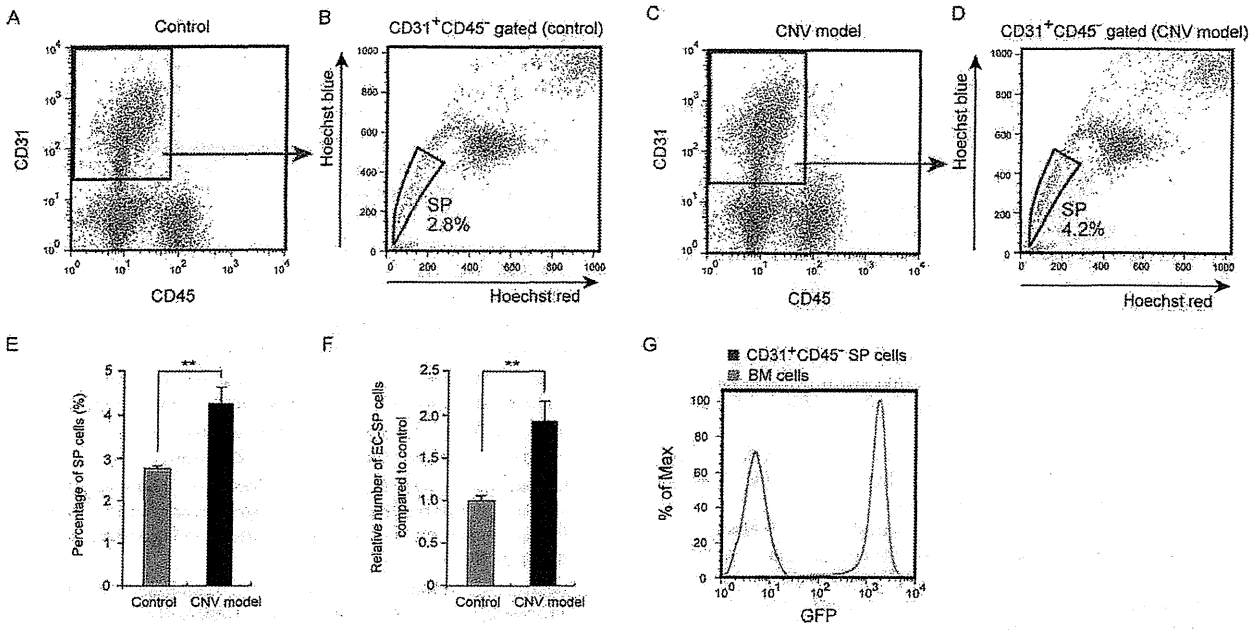

FIGURE 6. Choroidal EC-SP cells proliferate in laser-induced CNV. (**A–D**) Flow cytometric analysis of Hoechst 33342 staining of $CD31^+CD45^-$ ECs from the sham-operated choroid (**A**, **B**) and the choroid in which CNV had been induced (**C**, **D**). (**E**, **F**) Quantitative evaluation of the percentage (**E**) and absolute number (**F**) of EC-SP cells from 12 eyes. *Error bars* are ±SEM. $^{**}P < 0.01$ ($n = 3$, 12 eyes for each experiment, experiments repeated 3 times). (**G**) BM cells from GFP mice were transplanted into lethally-irradiated wild-type mice and, 24 weeks thereafter, CNV was induced by the laser. Cells from the choroid were analyzed 6 days after the laser treatment. The histogram shows the GFP intensity of the choroidal $CD31^+CD45^-$ EC-SP fraction (*red*) and BM (*green*). Almost all BM cells were GFP-positive after transplantation. The GFP-positive $CD31^+CD45^-$ EC-SP cells were present at <0.01% of the total, suggesting no major contribution of BM cells to EC-SP cells.

CNV model,[22] we found that the proportion and absolute number of EC-SP cells increased during CNV. The EC-SP cells that proliferated did not contain any BM-derived cells. Those results, combined with in vitro proliferative potential of EC-SP cells, indicated that EC-SP cells may possess self-renewal ability, and proliferate upon exposure to angiogenic stimuli, produce a large number of ECs, and potentially contribute to new choroidal vessels. Further studies are needed to elucidate the molecular signature of EC-SP cells, and to investigate the distribution and definitive in situ contribution of EC-SP cells during CNV formation.

Although retinal and brain vessels also are associated with angiogenesis-related diseases, such as diabetic retinopathy, cerebral infarction, and brain tumors, preexisting stem cell-like ECs must be those that contribute mainly to neovascularization. Because of the high baseline proportion, and less stem cell-like potential of EC-SP cells in the retina and brain, not only the SP phenotype, but also more specific molecular markers still are required for identifying resident stem cell-like cells and their contribution to angiogenesis. Furthermore, the physiologic role of stem cell-like cells in maintaining blood vessels remains to be investigated.

The data presented in our study suggested a potential strategy to treat blood vessel-related diseases in the future. First, in ischemic diseases, EC-SP cells may be used for proangiogenic therapy providing large numbers of vascular ECs and new blood vessels to restore blood flow in the damaged tissue. Second, in pathologic neovascularization, limiting the involvement and contribution of EC-SP cells may be useful for antiangiogenic therapy.

In summary, we identified SP cells in the $CD31^+CD45^-$ EC fraction in the eye and brain. In the choroid, EC-SP cells may represent vessel-residing endothelial stem/progenitor cells contributing to angiogenesis in vitro and in vivo. Further studies to identify the molecules responsible for the presence and proliferative potential of EC-SP cells may offer better understanding of the mechanism of angiogenesis, and development of new strategies for angiogenesis-related vascular diseases.

Acknowledgments

The authors thank Noriko Fujimoto and Chie Takeshita for cell preparation, and Keisho Fukuhara for administrative assistance.

Supported by Banyu Life Science Foundation International (HN), Grant-in-Aid for Scientific Research from the Ministry of Education, Culture, Sports, Science, and Technology, and Japan Society for the Promotion of Science of Japan (NT). The authors alone are responsible for the content and writing of the paper.

Disclosure: **T. Wakabayashi**, None; **H. Naito**, None; **K. Takara**, None; **H. Kidoya**, None; **S. Sakimoto**, None; **Y. Oshima**, None; **K. Nishida**, None; **N. Takakura**, None

References

1. Kempen JH, O'Colmain BJ, Leske MC, et al. Eye Diseases Prevalence Research Group. The prevalence of diabetic retinopathy among adults in the United States. *Arch Ophthalmol.* 2004;122:552–563.
2. Bressler NM. Age-related macular degeneration is the leading cause of blindness. *JAMA.* 2004;291:1900–1901.
3. Friedman DS, O'Colmain BJ, Munoz B, et al. Eye Diseases Prevalence Research Group. Prevalence of age-related macular degeneration in the United States. *Arch Ophthalmol.* 2004; 122:564–572.
4. Risau W. Mechanisms of angiogenesis. *Nature.* 1997;386:671–674.

5. Asahara T, Murohara T, Sullivan A, et al. Isolation of putative progenitor endothelial cells for angiogenesis. *Science*. 1997; 275:964–967.
6. Asahara T, Takahashi T, Masuda H, et al. VEGF contributes to postnatal neovascularization by mobilizing bone marrow-derived endothelial progenitor cells. *EMBO J.* 1999;18:3964–3972.
7. Grant MB, May WS, Caballero S, et al. Adult hematopoietic stem cells provide functional hemangioblast activity during retinal neovascularization. *Nat Med.* 2002;8:607–612.
8. Chan-Ling T, Baxter L, Afzal A, et al. Hematopoietic stem cells provide repair functions after laser-induced Bruch's membrane rupture model of choroidal neovascularization. *Am J Pathol.* 2006;168:1031–1044.
9. Okuno Y, Nakamura-Ishizu A, Kishi K, Suda T, Kubota Y. Bone marrow-derived cells serve as proangiogenic macrophages but not endothelial cells in wound healing. *Blood.* 2011;117: 5264–5272.
10. Grunewald M, Avraham I, Dor Y, et al. VEGF induced adult neovascularization: recruitment, retention, and role of accessory cells. *Cell.* 2006;124:175–189.
11. Rinkevich Y, Lindau P, Ueno H, Longaker MT, Weissman IL. Germ-layer and lineage-restricted stem/progenitors regenerate the mouse digit tip. *Nature.* 2011;476:409–413.
12. Purhonen S, Palm J, Rossi D, et al. Bone marrow-derived circulating endothelial precursors do not contribute to vascular endothelium and are not needed for tumor growth. *Proc Natl Acad Sci U S A.* 2008;105:6620–6625.
13. Naito H, Kidoya H, Sakimoto S, Wakabayashi T, Takakura N. Identification and characterization of a resident vascular stem/progenitor cell population in preexisting blood vessels. *EMBO J.* 2012;31:842–855.
14. Goodell MA, Brose K, Paradis G, Conner AS, Mulligan RC. Isolation and functional properties of murine hematopoietic stem cells that are replicating in vivo. *J Exp Med.* 1996;183: 1797–1806.
15. Challen GA, Little MH. A side order of stem cells: the SP phenotype. *Stem Cells.* 2006;24:3–12.
16. Golebiewska A, Brons NH, Bjerkvig R, Niclou SP. Critical appraisal of the side population assay in stem cell and cancer stem cell research. *Cell Stem Cell.* 2011;8:136–147.
17. Sakimoto S, Kidoya H, Naito H, et al. A role for endothelial cells in promoting the maturation of astrocytes through the apelin/APJ system in mice. *Development.* 2012;139:1327–1335.
18. Kidoya H, Ueno M, Yamada Y, et al. Spatial and temporal role of the apelin/APJ system in the caliber size regulation of blood vessels during angiogenesis. *EMBO J.* 2008;27:522–534.
19. Takakura N, Huang XL, Naruse T, et al. Critical role of the TIE2 endothelial cell receptor in the development of definitive hematopoiesis. *Immunity.* 1998;9:677–686.
20. Naito H, Takara K, Wakabayashi T, et al. Changes in blood vessel maturation in the fibrous cap of the tumor rim. *Cancer Sci.* 2012;103:433–438.
21. Kidoya H, Kunii N, Naito H, et al. The apelin/APJ system induces maturation of the tumor vasculature and improves the efficiency of immune therapy. *Oncogene.* 2012;31:3254–3264.
22. Ryan SJ. Subretinal neovascularization: natural history of an experimental model. *Arch Ophthalmol.* 1982;125:71–80.
23. Dean M, Fojo T, Bates S. Tumour stem cells and drug resistance. *Nat Rev Cancer.* 2005;5:275–284.
24. Tachikawa M, Toki H, Tomi M, Hosoya K. Gene expression profiles of ATP-binding cassette transporter A and C subfamilies in mouse retinal vascular endothelial cells. *Microvasc Res.* 2008;75:68–72.
25. Tagami M, Kusuhara S, Honda S, Tsukahara Y, Negi A. Expression of ATP-binding cassette transporters at the inner blood-retinal barrier in a neonatal mouse model of oxygen-induced retinopathy. *Brain Res.* 2009;1283:186–193.
26. Tomita M, Yamada H, Adachi Y, et al. Choroidal neovascularization is provided by bone marrow cells. *Stem Cells.* 2004;22: 21–26.
27. Sengupta N, Caballero S, Mames RN, Butler JM, Scott EW, Grant MB. The role of adult bone marrow-derived stem cells in choroidal neovascularization. *Invest Ophthalmol Vis Sci.* 2003;44:4908–4913.
28. Espinosa-Heidmann DG, Caicedo A, Hernandez EP, Csaky KG, Cousins SW. Bone marrow-derived progenitor cells contribute to experimental choroidal neovascularization. *Invest Ophthalmol Vis Sci.* 2003;44:4914–4919.
29. Zhang ZG, Zhang L, Jiang Q, Chopp M. Bone marrow-derived endothelial progenitor cells participate in cerebral neovascularization after focal cerebral ischemia in the adult mouse. *Circ Res.* 2002;90:284–288.

Investigative Ophthalmology & Visual Science

＜原　著＞

血管腫・血管奇形の全国疫学調査に向けての予備調査結果の報告
―重症度と難治性の分析―

力久直昭[*1]・小坂健太朗[*2]・松井裕輔[*3]・三村秀文[*4]
大須賀慶悟[*5]・秋田定伯[*6]・渡部　茂[*7]・佐々木　了[*8]

An Epidemiological Survey of Vascular Tumors and Vascular Malformations in Five Hospitals: an Analysis of Their Severity and Obstinacy

Naoaki RIKIHISA[*1], Kentaro KOSAKA[*2], Yusuke MATSUI[*3], Hidefumi MIMURA[*4], Keigo OSUGA[*5], Sadanori AKITA[*6], Shigeru WATANABE[*7] and Satoru SASAKI[*8]

[*1] *Department of Plastic Surgery, Chiba Rosai Hospital, Chiba, 290-0003*
[*2] *Department of Plastic, Reconstructive and Aesthetic Surgery, Chiba University Hospital, Chiba, 260-8677*
[*3] *Department of Radiology, Okayama University Graduate School of Medicine, Dentistry and Pharmaceutical Sciences, Okayama, 700-8558*
[*4] *Department of Diagnostic Radiology 2, Kawasaki Medical School, Okayama, 701-0192*
[*5] *Department of Diagnostic and Interventional Radiology, Osaka University Graduate School of Medicine, Osaka, 565-0871*
[*6] *Division of Plastic and Reconstructive Surgery, Department of Developmental and Reconstructive Medicine, Nagasaki University, Nagasaki, 852-8501*
[*7] *Department of Diagnostic Radiology 1, Kawasaki Medical School, Okayama, 701-0192*
[*8] *Center for Vascular Anomalies, KKR Sapporo Medical Center Tonan Hospital, Hokkaido, 060-0001*

和文要旨

厚生労働省難治性疾患等克服研究事業「難治性血管腫・血管奇形についての調査研究」班は，血管腫・血管奇形の実態を明らかにし難病としての施策に役立てる基盤形成を研究の目的としている。今回，班員の所属する5施設おいて2011年に診療した血管腫・血管奇形症例について疫学的調査を行った。主治医が難治性であると判断した症例は全体の42.0%を占め，研究班の作成した「血管腫・血管奇形重症度分類素案」で重症と診断された症例は全体の4.7%だった。このことから難治性症例が必ずしも重症例でないことが示された。この疾患群が医療費助成の対象疾患に選定されるためには，難治性と重症度について明確な基準を策定し，さらに難治性と重症の2つの要素を満たす症例数を適正な人数に近づけることが必要であることが分かった。今回の疫学的調査は予備調査であり，この結果を踏まえたわが国初の全国調査を今後行う予定である。

Key Words：血管腫・血管奇形，多施設調査，重症度，難治性，難病

[*1] 千葉労災病院形成外科　[*2] 千葉大学医学部附属病院形成美容外科　[*3] 岡山大学大学院医歯薬学総合研究科放射線医学
[*4] 川崎医科大学放射線医学（画像診断2）　[*5] 大阪大学大学院医学系研究科放射線医学　[*6] 長崎大学医学部形成外科学
[*7] 川崎医科大学放射線医学（画像診断1）　[*8] KKR札幌医療センター斗南病院血管腫・血管奇形センター

2013年5月21日受領
2013年6月20日掲載決定

英文アブストラクト

We, the study group of the Ministry of Health, Labour and Welfare, are conducting research to determine the actual situation of patients with vascular anomalies in Japan. Our research will provide a foundation for measuring the medical expense aid provided for the management of intractable diseases in Japan. We conducted an epidemiological survey among patients with vascular anomalies in five hospitals. Among the total of 343 patients, 42% of the patients were diagnosed with intractable diseases and 4.7% were severely disabled, as per our original severity-grading scale scores. On the basis of this result, it is clear that, if a patient is diagnosed with an intractable disease, it does not necessarily imply that he/she has severe impairment. We should design well-defined criteria for obstinacy and severity of such diseases so that patients with vascular anomalies are chosen as new recipients of extended medical expense aid. Thus, we will conduct the first national survey to determine the actual situation of patients with vascular anomaly in Japan.

Key Words：vascular tumors and vascular malformations, multicenter survey, severity, obstinacy, intractable disease

序　文

厚生労働省の難病対策委員会は2013年1月17日，難病対策の見直しと新法制化に向けた最終報告案をまとめた。医療費助成の対象疾患を現在の56から300疾患以上に増やす予定で，来年度以降の成立を目指す新法の制定後の政令で新たな対象疾患が決まる。

血管腫・血管奇形の発生頻度に関する国内での報告はなく，海外でも詳しい実態調査は行われていない。厚生労働科学研究費補助金難治性疾患等克服研究事業（難治性疾患克服研究事業）「難治性血管腫・血管奇形についての調査研究」（平成24年度 研究者代表：三村秀文）の研究班は，患者実態調査と治療方法の研究を行っている。血管腫・血管奇形の実態を明らかにし，難病としての施策に役立てる基盤形成を研究目的のひとつとしている。全国調査によって施策実行のための基本的データの収集を計画しているが，その前のパイロットスタディとして，研究班員の所属する複数施設を対象とした予備調査を2012年11月・12月に行った。予備調査結果の概要と，その調査で使用した症例の重症度分類（**表1a, b**）について検討を行ったので報告する。

方　法

各施設での倫理委員会の承認を取得したのち，2012年11月から2ヵ月間に，研究班所属医師が対象患者のデータをWeb登録した。症例登録データは連結可能匿名化し，患者カルテ番号，氏名，匿名番号の対応表は各施設の担当者が管理した。Web登録システムは，本研究が倫理委員会で承認されたのちにISO 27001/ISMS認証（一般財団法人日本情報経済社会推進協会による情報セキュリティマネジメントに対する第三者適合性評価制度）を取得している業者に委託し，匿名化されたデータは研究班が保持した。

調査対象となった患者は，2011年1月～12月までの間に研究班5施設で診療を行った血管腫・血管奇形患者343例（男性130例，女性213例）であった。Web登録入力の負担を軽減するため乳児血管腫例，毛細血管奇形（いわゆる単純性血管腫）単独の症例は除外した。Web登録に参加した施設は長崎大学病院，大阪大学医学部附属病院，千葉大学医学部附属病院，川崎医科大学附属病院，川崎医科大学附属川崎病院の5施設であった。

Web登録を行ったデータは以下の項目とした。生年月，性別，初発時期，併存疾患，既往症，家族歴，病変のおもな占拠部位，病変の深さ，病変の大きさ（長径），受診時症状および既往症状，動静脈奇形の場合Schöbinger病期[1]，診断名，診断の根拠，診断に有用だった画像診断，治療歴と治療回数（手術・硬化療法・塞栓術・レーザー治療・保存療法の有無），入院回数，治療の転帰，難治性か否か（主治医判断），血管腫・血管奇形の重症度（**表1a, b**）についてデータを収集した。

「血管腫・血管奇形の重症度分類」（**表1a, b**）は難治性血管腫・血管奇形についての研究班が議論を重ね作成したもので，整容面11項目，機能面15項目について，それぞれ1～5度の分類基準を設定している。各症例について，これら26項目について当てはまる症状をすべてWeb上で選択登録し，そのうち最大値をその患者の重症度とするシステムを構築した。

収集したデータを「重症度」と「難治性か否か（主治医判断）」に着目して分析し，重症例の臨床的な特徴，難治性症例の臨床的特徴について検討した。各項目をPearsonのχ^2検定またはMann-WhitneyのU検定を用いて検定した。

表1（a） 血管腫・血管奇形重症度分類（整容面）

部位			1度	2度	3度	4度	5度
露出面	顔ほう	頭部（頭髪部も含む）	手掌大2分の1未満の醜状	手掌大未満の醜状	手掌大以上の醜状	手掌大の2倍以上の醜状	
		顔面・頸部（眉毛部も含む）	顔面部にあっては，手掌大の4分の1未満の醜状 頸部にあっては，手掌大2分の1未満の醜状	顔面部にあっては，手掌大の4分の1以上の醜状 頸部にあっては，手掌大の2分の1以上の醜状	顔面部にあっては，手掌大の2分1以上の醜状 頸部にあっては，手掌大以上の醜状	顔面部にあっては，その2分の1程度をこえる醜状 頸部にあっては，その4分の3程度をこえる醜状	
		眼瞼	片側の上または下眼瞼の一部の輪郭の変形	片側の上または下眼瞼の2分の1程度をこえる輪郭の変形	片側の上または下眼瞼のほぼ全体に及ぶ輪郭の変形	片側の上および下眼瞼のほぼ全体にわたる輪郭の変形	
		口唇	上または下口唇それぞれの一部の輪郭の変形	上または下口唇の2分の1程度をこえる輪郭の変形	上または下口唇のほぼ全体に及ぶ輪郭の変形	上および下口唇のほぼ全体にわたる輪郭の変形	
		鼻	鼻部の一部の輪郭の変形	鼻部の4分の1程度をこえる輪郭の変形	鼻部の2分の1程度をこえる輪郭の変形	鼻部の全体に及ぶ輪郭の変形	
		耳	片側耳介軟骨部の4分の1程度をこえる輪郭の変形	片側耳介軟骨部の2分の1程度をこえる輪郭の変形	片側耳介軟骨部のほぼ全体にわたる輪郭の変形		
	四肢の露出面	手部	手掌部の3分の1程度をこえない醜状 手背部の4分の1程度をこえない醜状	手掌部の3分の2程度をこえない醜状 手背部の2分の1程度をこえない醜状	手掌部の3分の2程度をこえる醜状 手背部の2分の1程度をこえる醜状 左右同じ手袋がはめられない		
		上肢（前腕節以下手関節以上）	一上肢にある手掌大の2倍未満の醜状 直立自然位で左右の上肢長差が手掌の長さの半分未満のもの 左右の前腕または上腕の周径差が最大の部位において，その差が健常側の周囲長の3割未満のもの	一上肢にある手掌大の2倍以上の醜状 直立自然位で左右の上肢長差が手掌の長さ未満のもの 左右の前腕または上腕の周径差が最大の部位において，その差が健常側の周囲長の3割以上のもの	一上肢にある一上肢の全面積の2分の1程度をこえる醜状 直立自然位で左右の上肢長差が手掌の長さ以上異なるもの 左右の前腕または上腕の周径差が最大の部位において，その差が健常側の周囲長の5割以上のもの	一上肢の上腕かつ前腕の深部組織（皮下組織・筋肉・骨）に病変が広く存在するもの	
		膝関節以下の下肢（足部を含む）	膝関節以下一下肢にある手掌大未満の醜状 左右の下腿の周径差が最大の部位において，その差が健常側の周囲長の2割未満のもの	膝関節以下の一下肢にある手掌大以上の醜状 左右の下腿の周径差が最大の部位において，その差が健常側の周囲長の2割以上のもの 左右の趾の長さ・周囲長が異なる	膝関節以下の一下肢にある手掌大の2倍以上の醜状 左右同じ靴が履けない 左右の下肢長差が3cm未満 左右の下腿の周径差が最大の部位において，その差が健常側の周囲長の3割以上のもの	片側の膝関節以下に，その全面積の2分の1程度をこえる醜状を呈するもの 長管骨の変形 左右の下肢長差3cm～5cm 左右の下腿の周径差が最大の部位において，その差が健常側の周囲長の4割以上のもの 一下肢の大腿かつ下腿の深部組織（皮下組織・筋肉・骨）に病変が広く存在するもの	片側の膝関節以下に，そのほぼ全面積に及ぶ醜状を呈するもの 長管骨の著しい変形 左右の下肢長差が5cm以上 左右の下腿の周径差が最大の部位において，その差が健常側の周囲長の5割以上のもの
非露出面		体幹・生殖器	胸腹部または背部・殿部にあってその全面積の4分の1程度をこえない程度の醜状	体幹輪郭の軽度変形 胸腹部または背部・殿部にあってその全面積の4分の1程度をこえる醜状	胸腹部または背部・殿部にあってその全面積の2分の1程度をこえる醜状	骨（脊椎・肋骨・鎖骨・胸骨・骨盤骨）の変形を伴う醜状	骨（脊椎・肋骨・鎖骨・胸骨・骨盤骨）の著しい変形を伴う醜状
		膝関節以上の下肢（大腿）	左右の大腿の周径差が最大の部位において，その差が健常側の周囲長の2割未満のもの 片側の大腿の2分の1程度をこえない醜状	左右の大腿の周径差が最大の部位において，その差が健常側の周囲長の2割以上のもの 片側の大腿の2分の1程度をこえる醜状	左右の大腿の周径差が最大の部位において，その差が健常側の周囲長の3割以上のもの 左右の下肢長差が3cm未満 片側の大腿のほとんど全域に及ぶ醜状	長管骨の変形 左右の下肢長差3cm～5cm 左右の大腿の周径差が最大の部位において，その差が健常側の周囲長の4割以上のもの 一下肢の大腿かつ下腿の深部組織（皮下組織・筋肉・骨）に病変が広く存在するもの	長管骨の著しい変形 左右の下肢長差が5cm以上 左右の大腿の周径差が最大の部位において，その差が健常側の周囲長の5割以上のもの

表1（b）　血管腫・血管奇形重症度分類（機能面とその他）

部位			1度	2度	3度	4度	5度
露出面	顔ぼう	中枢神経機能・末梢神経機能（疼痛を含む）	神経系統の機能または精神に障害を残すが，2度を満たさない程度のもの	神経系統の機能または精神に障害を残し，服することができる作業がある程度に制限されるもの	神経系統の機能または精神に障害を残し，服することができる作業が相当な程度に制限されるもの	神経系統の機能または精神に障害を残し，軽易な作業以外の作業に服することができないもの	神経系統の機能または精神に著しい障害を残し，特に軽易な作業以外の作業に服することができないもの 中等度から高度の強さの痛みに用いるオピオイド鎮痛薬の使用によって初めて鎮痛が得られるもの，またはそれらを使用しても鎮痛が十分得られないもの（小児例も含む）
		眼瞼・眼球	一眼の視力が0.6以下になったもの 一眼に半盲症，視野狭窄または視野変状を認めるもの 正面視以外で複視を認めるもの	一眼の眼球に著しい調節機能障害または運動障害を認めるもの 一眼の上眼瞼に著しい運動障害を認めるもの 一眼の視力が0.1以下になったもの	両眼の視力が0.6以下になったもの 一眼の視力が0.06以下になったもの 正面視で複視を認めるもの 両眼の眼球に著しい調節機能障害または運動障害を認めるもの 両眼の上眼瞼に著しい運動障害を認めるもの	一眼が失明し，一眼の視力が0.6以下になったもの 両眼に半盲症，視野狭窄または視野変状を認めるもの	両眼の視力が0.1以下になったもの
		呼吸機能・心機能	病変が原因となり閉塞型睡眠時無呼吸症候群をきたすが，日中の傾眠傾向がないもの	病変が原因となり閉塞型睡眠時無呼吸症候群をきたし，自分の意志に反し眠気があり，気づかずに眠ってしまうことがあまり集中していないときに起こるもの	病変が原因となり閉塞型睡眠時無呼吸症候群をきたし，自分の意志に反し眠気があり，気づかずに眠ってしまうことが，多少集中を必要としているとき起こるもの，症状により社会的にあるいは仕事上の機能に中等度の障害が起こるもの 身体活動には特に制約がなく日常労作により，特に不当な呼吸困難，狭心痛，疲労，動悸などの愁訴が生じないが，検査上異常が指摘され第4度への移行が懸念されるもの	病変が原因となり閉塞型睡眠時無呼吸症候群をきたし，自分の意志に反し眠気があり，気づかずに眠ってしまうことが，強い集中を必要としているとき起こるもの，症状により社会的にあるいは仕事上の機能に高度の障害が起こるもの 安静時または軽労作時には障害がないが，日常労作のうち，比較的強い労作（たとえば，階段上昇，坂道歩行など）によって，呼吸困難，狭心痛，疲労，動悸などの愁訴が生じるもの 気管切開（気管孔作成）が施行されているもの	病変が原因となり閉塞型睡眠時無呼吸症候群をきたし，身体活動に高度の制約のあるもの 安静時には無症状であるが，普通以下の軽労作で呼吸困難，狭心痛，疲労，動悸などの愁訴を生じるもの
		咀嚼機能・嚥下機能		咀嚼機能・嚥下機能に軽度の障害を認めるが，3度の条件は満たさない程度のもの	ある程度の常食は摂取できるが，咀嚼・嚥下が十分できないために食事が制限される程度のもの	経口摂取のみでは十分な栄養摂取ができないため，経管栄養の併用が必要なもの 全粥または軟菜以外は摂取できない程度のもの	流動食以外は摂取できない程度のもの 経口的に食物を摂取することができないもの 食物が口からこぼれ出るため，常に手や器物などでそれを防がなければならない程度のもの 経口的な食物摂取がきわめて困難で1日の大半を食事に費やさなければならない程度のもの
		構音機能		構音機能に軽度の障害を認めるが，3度の条件は満たさない程度のもの	電話による会話が，家族は理解できるが他人には理解できない程度のもの	日常会話が，家族は理解できるが他人には理解できない程度のもの	日常会話が，誰が聞いても理解できない程度のもの
		鼻			鼻の機能に著しい障害を認めるもの		
		耳	一耳の聴力が1m以上の距離では普通の話声を解することができない程度の難聴になったもの	両耳の聴力が1m以上の距離では小声を解することが困難な程度の難聴になったもの 一耳の聴力が40cm以上の距離では普通の話声を解することができない程度の難聴になったもの	両耳の聴力が1m以上の距離では普通の話声を解することが困難な程度の難聴になったもの 一耳の聴力が耳に接しなければ大声を解することができない程度の難聴になったもの 一耳の聴力を全く失ったもの	両耳の聴力が40cm以上の距離では普通の話声を解することが困難な程度の難聴になったもの 一耳の聴力を全く失い，他耳の聴力が1m以上の距離では普通の話声を解することができない程度の難聴になったもの	一耳の聴力を全く失い，他耳の聴力が40cm以上の距離では普通の話声を解することができない程度の難聴になったもの 両耳の聴力が耳に接しなければ大声を解することができない程度以上の難聴になったもの

四肢の露出面	手部・上肢	一手の示指，中指，環指または小指の用を廃したもの 母指以外の手指の遠位指節間関節を屈伸することができなくなったもの 一上肢の三大関節中の一関節の機能に障害を認めるもの	一手の母指または母指以外の二手指の用を廃したもの 一上肢の三大関節中の一関節の機能に著しい障害を認めるもの	一手の母指を含み三手指または母指以外の四手指の用を廃したもの 一上肢の三大関節中の一関節の用を廃したもの	手の五手指または母指を含み四手指の用を廃したもの 一上肢の三大関節中の二関節の用を廃したもの	一上肢の用を全廃したもの（三大関節の用を廃したもの）
	膝関節以下の下肢（足部を含む）	一足の第三足指以下の一または二の足指の用を廃したもの	一足の第一または第二足指を含み一以上の足指の用を廃したもの 一下肢の膝関節・足関節のうちの一関節の機能に障害を認めるもの	一足の足指の全部の機能を廃したもの 一下肢の膝関節・足関節のうちの一関節の機能に著しい障害を認めるもの	一下肢の膝関節・足関節のうちの一関節の用を廃したもの	一下肢の膝関節と足関節の用を廃したもの
非露出面	体幹・生殖器	胸腹部臓器の機能に障害を認めるもの 局部に神経症状を認めるもの	胸腹部臓器の機能に障害を残し，服することができる作業がある程度に支障があるもの 局部に頑固な神経症状を認めるもの	胸腹部臓器の機能に障害を残し，服することができる作業が相当な程度に制限されるもの 立位・座位の保持に支障があるもの 生殖器に著しい障害を認めるもの	胸腹部臓器の機能に障害を残し，軽易な作業以外の作業に服することができないもの 立位・座位の保持が相当な程度に制限されるもの 脊柱に運動障害を認めるもの 両側の睾丸または卵巣の機能を失ったもの	胸腹部臓器の機能に著しい障害を残し，特に軽易な作業以外の作業に服することができないもの 立位・座位の保持ができないもの 脊柱に著しい運動障害を認めるもの
	膝関節以上の下肢（大腿）		一下肢の股関節の機能に障害を認めるもの	一下肢の股関節の機能に著しい障害を認めるもの	一下肢の股関節の用を廃したもの	一下肢の股関節と膝関節または足関節の用を廃したもの
出血および出血の可能性		ときおり出血するが医療的処置の必要のないもの	しばしば出血するが医療的処置の必要のないもの	出血の治療ため医療的処置を必要とするが，治療によって出血予防・止血が十分に得られるもの	致死的な出血のリスクをもつもの 複数年にわたり出血の治療のため1年間に1回程度の入院加療を要したあるいは要す見込みのもの 慢性出血性貧血のため月1回程度の輸血を定期的に必要とするもの	致死的な出血のリスクが非常に高いもの 大量出血のリスクが高く年間30日以上の入院治療が必要なもの 複数年にわたり出血の治療のため1年間に2回以上入院加療を要したあるいは要す見込みのもの
感染および感染の可能性			しばしば感染を併発するが医療的処置の必要のないもの	感染・蜂窩織炎の治療のため医療的処置を必要とするが，治療によって十分に症状の進行を抑制できるもの	敗血症などの致死的な感染を合併するリスクをもつもの 複数年にわたり感染・蜂窩織炎の治療のため1年間に1回程度の入院加療を要したあるいは要す見込みのもの	敗血症などの致死的な感染を合併するリスクが非常に高いもの 感染・蜂窩織炎のリスクが高く年間30日以上の入院治療が必要なもの 複数年にわたりの感染・蜂窩織炎の治療のため1年間に2回以上入院加療を要したあるいは要す見込みのもの
難治性皮膚潰瘍		難治性皮膚潰瘍の治療・保護する必要はあるが，2度を満たさない程度のもの	難治性皮膚潰瘍の治療・保護のため，服することができる作業がある程度に制限されるもの	難治性皮膚潰瘍の治療・保護のため，服することができる作業が相当な程度に制限されるもの	難治性皮膚潰瘍の治療・保護のため，軽易な作業以外の作業に服することができないもの	難治性皮膚潰瘍の治療・保護のため，特に軽易な作業以外の作業に服することができないもの
凝固能異常				血液検査データでは凝固能異常を示すが，出血傾向などの臨床症状を伴わないもの	凝固能異常に対して治療を必要とするが，医療的処置によって出血傾向などの臨床症状の改善を得ることができるもの	凝固能異常に対して治療を必要とし，医療的処置を行っても出血傾向などの臨床症状が改善しないもの